Nuclear Quadrupole Coupling in Transition Metal Compounds

by

Shen-Dat Ing

Thesis submitted to the Graduate Faculty of the

Virginia Polytechnic Institute and State University

in partial fulfillment of the requirements for the degree of

Doctor of Philosophy

in

Department of Chemistry

APPROVED:

Jack D. Graybeal, Chairman

Thomas C. Ward

Larry T. Taylor

Harold M. McNair

Ray F. Tipsword

November, 1971

Blacksburg, Virginia

TABLE OF CONTENTS

ACKNOWLEDGEMENTS

The author wishes to express his appreciation to his major professor, Dr. Jack D. Graybeal, for his patience and help during the courses of this investigation. He would also like to thank his parents for their constant encouragements and sacrifice, without that the task of this work would be impossible.

The financial support of the National Science Foundation, as well as the Chemistry Department at Virginia Polytechnic Institute and State University are both acknowledged with gratitude.

LIST OF TABLES

LIST OF FIGURES

INTRODUCTION

Since the first experiments regarding the properties of nuclei, much interest has been centered on the interaction between the nucleus and various environmental factors, particularly magnetic fields and electric fields. As a result of such studies it has been found that nuclei can possess magnetic dipole moments, electric quadrupole moments and higher multipole moments. The fact that some nuclei have an electric quadrupole moment that can interact with the surrounding electric field is the basis for nuclear quadrupole resonance (NQR) spectroscopy.

A nucleus in any molecular environment is surrounded by electrons and other nuclei. These electrons and nuclei are electrical in nature and result in the production of an electric field at the nuclear site. The electric quadrupole moment of the nucleus may then interact with the surrounding electric field in such a manner as to produce a discrete set of energy levels. Transitions between these levels may be observed directly by application of radio-frequency energy of the correct frequency. The frequencies of these observed transitions depend on the quadrupole moments of the nuclei and the electric field gradient (EFG) tensor components of the surrounding electric fields. Since the nuclear quadrupole moment is a constant for a particular nucleus, a knowledge of the EFG tensor components can be obtained experimentally. These in turn can be correlated with the electronic distribution in the molecule and hence with the type of bonding occuring in the molecule. In this light, the quadrupole moment serves as a probe for

examining the internal electronic configuration of a molecule or of a crystalline solid. Elucidation of the bonding properties of atoms in solids may be afforded by judicious interpretation of the results of such experiments.

The study of insertion reactions by inserting metal containing groups into the $Co_2(CO)_8$ to form a metal-metal covalent bond was initiated by Graham[35]. Infrared and nuclear magnetic resonance studies on these compounds have shown definite trends in the infrared stretching frequencies, the intensity of the infrared spectra and the NMR coupling constants. Since the observed NQR frequency of a particular Co nucleus is sensitive to the local electronic environment a knowledge of the NQR frequencies and the electric field gradient tensor components derivable from it can be correlated with the electronic distribution in the molecule and hence with the type of bonding occuring in the molecule. A correlation between the findings of NQR studies and those of IR and NMR can further the understanding of the nature of bonding in these compounds.

^{63}Cu and ^{65}Cu NQR resonance frequencies in Cu_2O and $KCu(CN)_2$ were reported in the early 1950's. Since then, no other copper resonances have been reported. The reported resonance frequencies for both compounds were within the range of the available spectrometer so this area constituted an open field for exploration. Due to the inherent broadening of NQR transitions by the presence of a paramagnetic species investigations of Cu NQR frequencies were restricted to Cu(I) compounds. A series of Copper(I) thiourea and substituted

thiourea complexes were chosen for investigation. These studies were directed toward learning more about the nature of the bonding in these compounds.

In an effort to extend the use of NQR to new systems several molybdenum compounds were investigated. Resonances which are attributable to Mo nuclei were observed but precise assignment to a particular isotopic species is impossible due to limitations on the operating range of the spectrometer. The limited number of observations severely restrict the relationship of the observed frequencies to bonding properties.

REVIEW OF THEORETICAL CONCEPTS

A). NQR Energy Levels and Transitions.

The theory of nuclear quadrupole coupling in both atoms and molecules has been extensively discussed in several general monographs[7,12,27,54]. In this section we will present a brief review of those aspects of the theory which are of particular applicability to the studies discussed in this dissertation. The discussion will thus be limited to interactions in solids, nuclei of half integer spin, and the case of no external magnetic field.

When a crystal containing an electrically asymmetric nucleus is placed in an oscillating magnetic field it may absorb magnetic energy at certain frequencies determined by the electrical interaction of the nucleus with its surroundings. With an asymmetric nucleus the important electrical interaction is expressed as a product of the gradient of the electric field at the nucleus and the quadrupole moment of the nucleus. This interaction is known as nuclear quadrupole coupling. The Hamiltonian, H, describing the interaction between a nucleus and the surrounding electronic charge may be written as

$$H = \int_{V_e} \int_{V_n} \frac{P_e(r_e)P_n(r_n)dV_e dV_n}{r} \qquad (1)$$

where $P_e(\mathbf{r}_e)$ is the charge density external to the nucleus in the volume element dV_e at position $\mathbf{r}_e$ with respect to the center of the nucleus and $P_n(V_n)$ is the charge density of the volume element dV_n

within the nucleus at a position $\mathcal{R}_n$ with respect to the center of the nucleus. The vector $\mathcal{R}_n$ is from dV_n to dV_e and θ_{en} is the angle between $\mathcal{R}_e$ and $\mathcal{R}_n$ as shown in Figure 1. By employing the law of cosines

$$\frac{1}{r} = (r_e^2 + r_n^2 + 2r_e r_n \text{Cos } \theta_{en})^{-1/2} \tag{2}$$

or

$$\frac{1}{r} = (1 + (\frac{r_n}{r_e})^2 - 2\frac{r_n}{r_e} \text{Cos } \theta_{en})^{1/2} \frac{1}{r_e} \tag{3}$$

and expanding Equation (3) in a power series in $\frac{\mathcal{R}_n}{\mathcal{R}_e}$, one obtains

$$\frac{1}{r} = \frac{1}{r_e} \left[1 + \frac{r_n}{r_e} P_1 + (\frac{r_n}{r_e})^2 P_2 + \ldots . \right] \tag{4}$$

where P_e is the Legendre polynomial, i.e.,

$$P_1 = \text{Cos } \theta_{en}$$
$$P_2 = \frac{1}{2} (3 \text{Cos}^2 \theta_{en} - 1) \tag{5}$$

etc.

Substitution of Equation (4) into equation (1) results in a series of terms, the first corresponding to the interaction of the surrounding field with the nuclear charge, the second corresponding to the interaction of the field with the nuclear electric dipole moment and the third corresponding to an interaction of the field with the nuclear electric quadrupole moment. The third term is the one of interested in this study. In general a term in P_ℓ corresponds to a multipole moment of 2^ℓ. The expression resulting from substituting Equations (4) and (5) into equation (1) is,

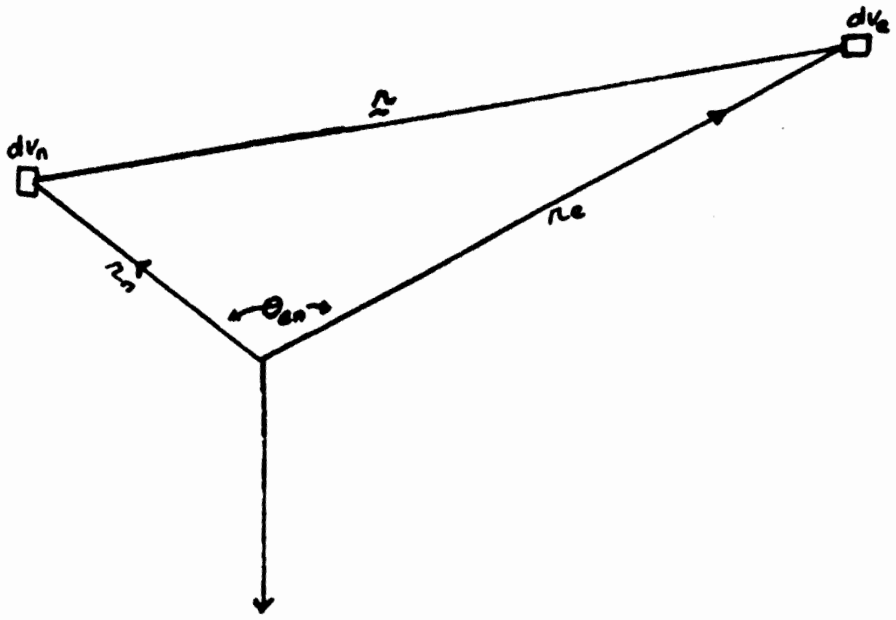

Figure 1

Vectorial Representation of Nuclear
Quadrupole Coupling

$$H_Q = \int_{V_e} \int_{V_n} V_n^2 P_n \tfrac{1}{2} \left[3\cos^2\theta_{en} - 1 \quad P_e(r_e)/V_e^3 \right] dV_n dV_e \qquad (6)$$

One must point out here that the condition for the use of the power series expansion to derive equation (4) is that $r_n < r_e$. Equation (6) therefore is valid only if this same condition is fulfilled. As a consequence of this condition, we have in effect excluded all electronic charges which penetrate the nucleus. Such an exclusion, however, does not pose a serious problem. It is known that only s-electrons have a non-zero probability of penetrating the nucleus, and because of their spherically symmetric distribution they produce no observable interaction with the nuclear electric quadrupole moment. One may reexpress Equation (6) in terms of cartesian coordinates by using the relationship

$$r_e r_n \cos\theta_{en} = \sum_i X_{ei} X_{ni} \qquad (7)$$

to yield

$$H_Q = \int_{V_n} P_n(r_n)(3X_{ni}X_{nj} - \delta_{ij} r_n^2)\, dV_n \qquad (8)$$

However, if one defines Q_{ij} and $(E)_{ij}$ by the relationships

$$Q_{ij} = \int_{V_n} P_n(r_n)(3X_{ni}X_{nj} - \delta_{ij} r_n^2) dV_n \qquad (9)$$

$$= \int_{V_n} P_n(r_n) \left[\frac{(X_{ni}X_{nj} + X_{nj}X_{ni})}{2} - \delta_{ij} r_n \right] dV_n$$

and

$$(\nabla E)_{ij} = - \int_{V_e} P_e(r_e) \frac{\partial}{\partial X_i} \frac{\partial}{\partial X_j} \left(\frac{1}{r_e}\right) d V_e \qquad (10)$$

$$= - \int_{V_e} P_e(r_e) \left[\frac{3(X_{ei}X_{ej} + X_{ej}X_{ei})}{r_e^5} - \delta_{ij} r_e^2 \right] dV_e$$

Then,

$$H_Q = - \frac{1}{6} \sum_{ij} Q_{ij}(\nabla E)_{ij} = \overline{\overline{Q}} : \overline{\overline{\nabla E}} \qquad (11)$$

where the double dot indicates a scalar product of two second rank tensors. This may be verified by direct expansion of Equation (11) using the first form of Equation (9) and the second form of Equation (10). Equation (11) is the most generally used representation for H_Q. It consists of two tensors $\overline{\overline{Q}}$ (the quadrupole tensor) and $\overline{\overline{\nabla E}}$ (the electric field gradient tensor) whose elements Q_{ij} and $(\nabla E)_{ij}$ have been defined by Equations (9) and (10) respectively. By inspection of Equations (9) and (10) both $\overline{\overline{Q}}$ and $\overline{\overline{\nabla E}}$ can be shown to be traceless tensors.

The elements of the Q tensor can also be represented by the form[42]

$$Q_{ij} = C \left[3 \frac{I_i I_j + I_j I_i}{2} - \delta_{ij} \hat{I}^2 \right] \qquad (12)$$

where I_i and I_j are components of the nuclear spin operator I and C is a constant scalar quantity. The arbitrary constant C may be expressed in terms of a scalar nuclear quadrupole moment Q, which is a measure of the departure of the nuclear charge distribution from spherical symmetry. This scalar moment is defined by

$$Q \equiv \frac{1}{e} \int_{P_{n,m_{j=I}}} \left[3Z_n^2 - r_n^2 \right] dV_n \qquad (13)$$

$$
\begin{aligned}
(\nabla E)_o &= \tfrac{1}{2} V_{zz} \\
(\nabla E)_{\pm} &= -\tfrac{1}{\sqrt{6}} (V_{xz} \pm i\, V_{yz}) \\
(\nabla E)_{\pm 2} &= \tfrac{1}{2\sqrt{6}} (V_{xx} - V_{yy} \pm 2i\, V_{xy})
\end{aligned}
\tag{18}
$$

Any symmetric tensor may be transformed to a principal axis system and thus be diagonalized. The diagonalized tensor components are,

$$
\begin{aligned}
(\nabla E)_o &= \tfrac{1}{2} V_{zz} = \tfrac{1}{2} eq \\
(\nabla E)_{\pm 1} &= 0 \\
(\nabla E)_{\pm 2} &= \tfrac{1}{2\sqrt{6}} (V_{xx} - V_{yy}) = \tfrac{1}{2\sqrt{6}}\ eq
\end{aligned}
\tag{19}
$$

where

$$
\begin{aligned}
q &= \tfrac{1}{e} V_{zz} \\
\eta &= \frac{V_{xx} - V_{yy}}{V_{zz}}
\end{aligned}
\tag{20}
$$

By using the convention

$$
|V_{xx}| \leq |V_{yy}| \leq |V_{zz}| \tag{21}
$$

η may have values from 0 to 1. For $\eta = 0$,

$$
V_{xx} = V_{yy} = -\tfrac{1}{2} V_{zz} = \tfrac{1}{2} qe \tag{22}
$$

This corresponds to cylindrical (axial) symmetry about the z-axis of the principal axis system. For the case $\eta = 1$,

$$
\begin{aligned}
V_{xx} &= 0 \\
V_{zz} &= -V_{yy} = eq
\end{aligned}
\tag{23}
$$

where the subscript $m_I = I$ indicates the integral is carried out for the nuclear state with the magnetic quantum number $m_I = I$. It can also be defined by

$$Q = \frac{1}{C} (I,I|Q_{zz}|I,I) \tag{14}$$

where

$$\begin{aligned} \langle II|Q_{zz}|II\rangle &= C \langle II|3(I_z)^2 - I^2|II\rangle \\ &= C\left[3I^2 - I(I+1)\right] \\ &= C\ I\ (2J-1) \end{aligned} \tag{15}$$

therefore using Equation (12)

$$Q_{ij} = \frac{eQ}{I(2I-1)} \left[3\,\frac{I_i J_j + I_j I_i}{2} - \delta_{ij} I^2 \right] \tag{16}$$

At this point, it is of interest to point out that it is generally considered that nuclei with spin $I = 0, 1/2$ do not have quadrupole moments. This is incorrect however as Cook[4] has pointed out. Nuclei with $I = 0, 1/2$ can have quadrupole moments, but it is impossible to observe a nuclear electric multipole moment of order greater than 2^{ℓ} where $\ell = 2I$.

Let us now examine the electric field gradient tensor. The EFG tensor elements given by Equation (10) can be expressed in terms of the $V_{ij} = \frac{\partial V}{\partial X_i \partial X_j}$ where $\bar{V}$ is the electrostatic potential at the nucleus. The units of V_{ij} are cm^{-3}. Since $\bar{\bar{\nabla E}}$ is a traceless symmetric tensor and the Laplace condition

$$V_{xx} + V_{yy} + V_{zz} = 0 \tag{17}$$

must be satisfied,[7] there are 5 irreducible tensor components

The asymmetry parameter, η, is therefore a measure of the departure of the electric field from axial symmetry about the principal z-axis. Next we will relate the observed frequencies to the quantities q, and

The quadrupole energy level matrix elements will be

$$\langle m|H_Q|m'\rangle = \frac{eQq_{ij}}{6I(2I-1)}\sum\langle m|\frac{3}{2}I_iI_j + I_jI_i - \delta_{ij}I^2|m'\rangle \qquad (24)$$

where m takes the values m = I, I-1, ·····-I. Since

$$\langle m|I_z|m\rangle = m\,\delta_{mm'}$$
$$\langle m|I_x \pm iI_y|m'\rangle = \left[(Im)(I\mp(m+1))\right]^{1/2}\delta_{m\pm1,\,m'} \qquad (25)$$

where I_z, I_y, I_x designate the components of the spin angular momentum operator I, the only non-zero matrix elements become

$$\langle m|H_Q|m\rangle = \langle -m|H_Q|-m\rangle = \frac{e^2Qq}{I(2I-1)}\left[3m^2-I(I+1)\right] \qquad (26)$$

and

$$\langle m\pm2|H_Q|m\rangle = \frac{\sqrt{6}e\,Q}{4I(2I-1)}\left[(I\mp m)(I\mp m-1)(I\pm m+1)(I\pm m+2)\right]^{1/2}(\nabla E)\pm2 \qquad (27)$$

The energies of the quadrupolar states are then given by

$$E = \frac{e^2Qq}{4I(2I-1)}\;\frac{\eta}{2}\left[I(I+1)-m(m+1)\right]^{1/2}\left[(I+1)I-(m\pm1)(m\pm2)\right]^{1/2} \qquad (28)$$

The quantity e^2Qq is commonly known as the nuclear quadrupole coupling constant.

For an axially symmetry case, i.e. $\eta = 0$, the only non-zero matrix elements come from Equation (26) and the energies are given by

$$E_m = \langle m|H_Q|m\rangle = A\,[3m^2 - I(I+1)] \qquad (29)$$

where

$$A = \frac{e^2Qq}{4I(2I+1)}$$

Inspection of Equation (29) shows that all levels, except that one with m = 0, are doubly degenerate. Thus for half-integral spins there are I+1/2 energy levels and for integral spins there are I+1 energy levels.

In order to observe transitions between quadrupole energy levels one can in principle either apply an oscillating electric field, thereby producing an electric field gradients at the nucleus which would interact with the electric quadrupole moment of the nucleus or apply an oscillating magnetic field to obtain an interaction of the nuclear magnetic moment and the external oscillating magnetic field. The former method would require an electric field of 10^{14} volts/cm^2 [8]. This is too large to be practical. The second method is generally employed. Since the interaction involves an electromagnetic field a time-dependent Hamiltonian must be considered. The time-dependent Hamiltonian representing this interaction is given by[7]

$$H'(t) = -\gamma\hbar(H_xI_x + H_yI_y + H_zI_z) \qquad (30)$$

where γ is the magnetogyric ratio, h is Planck's constant, I_x, I_y, I_z the components of the angular momentum operator I, and H_x, H_y, H_z, the x, y, z - components of a linearly polarized oscillating electromagnetic field, 2H Cos wt. The transition probability which is proportional to the matrix element $\langle m|H'(t)|\, m'\rangle^2$ can therefore

be calculated with the aid of Equation (25). For the axially symmetric case, $\eta = 0$, the selection rules are $\Delta m = 0$, and $\Delta m = \pm 1$. For $\Delta m = 0$, transitions can be produced only by the z-component of the magnetic field and involve no change in energy and are of no interest here. For $\Delta m = \pm 1$, the maximum transition probability can occur only if the Bohr condition

$$w_m = \frac{(E_{m+1} - E_m)}{\hbar} \tag{31}$$

is satisfied.

The frequencies of the quadrupole transitions for the axially symmetric case are thus given by

$$w_m = \frac{E_{m+1} - E_m}{\hbar} = \frac{3A}{\hbar} (2m + 1) \tag{32}$$

Again there are $I - 1/2$ and $I - 1$ doubly degenerated levels for half integer and integer nuclear spin respectively. If I and m are known, then e^2Qq may be calculated from the measured absorption frequency. If m is not known, as is often the case for spin $I = 3/2$, the values of m_1 and m_2 may be uniquely determined by the ratio

$$\frac{w_1}{w_2} = \frac{2m_1 + 1}{2m_2 + 1} \tag{33}$$

For the case, $I = 3/2$, there is only one transition frequency which, when one assumes $\eta = 0$, is given by

$$w = \frac{E\pm 3/2 - E\pm 1/2}{\hbar} = \frac{6A}{\hbar} = \frac{e^2Qq}{2\hbar} \tag{34}$$

The problem of deriving expressions relating e^2Qq, η, and w, becomes much more complex for the non-axially symmetric case. The normal selection rules, $\Delta m = 0, \pm 1$, no longer hold. In fact, for values of $\eta > 0.1$, the probability for observation of transitions corresponding to $\Delta m = \pm 2$ becomes quite large[43]. This is because of mixing of the pure magnetic dipoles states differing in m by ± 2. We now not only have to consider the diagonal matrix elements $H_{mm} = \langle m|H_Q|m\rangle$ but also the off-diagonal elements $H_{m,\, m\pm2} = \langle m|H_Q|m\pm2\rangle$.

Thus for I = 3/2, the energy matrix has the form

$$H_Q = \begin{pmatrix} H_{3/2\ 3/2}-E & 0 & H_{3/2,-1/2} & 0 \\ 0 & H_{1/2\ 1/2}-E & 0 & H_{1/2,-3/2} \\ H_{-1/2,\ 3/2} & 0 & H_{-1/2-1/2}-E & 0 \\ 0 & H_{-3/2,\ 1/2} & 0 & H_{-3/2-3/2}-E \end{pmatrix} \quad (35)$$

where $H_{\pm3/2,\pm3/2} = 3A$, $H_{+1/2\pm1/2} = -3A$ and $H_{+1/2\pm3/2} = \sqrt{3}A\eta$.

Upon reordering of the columns and rows, this matrix has the form,

$$H_Q = \begin{pmatrix} H_{3/2\ 3/2}-E & H_{3/2,-1/2} & 0 & 0 \\ H_{-1/2,3/2} & H_{-1/2-1/2}-E & 0 & 0 \\ 0 & 0 & H_{1/2\ 1/2}-E & H_{+1/2-3/2} \\ 0 & 0 & H_{-3/2-1/2} & H_{-3/2-3/2}-E \end{pmatrix} \quad (36)$$

The matrix is thus factored into two identical submatrices which when solved given the energy levels,

$$E_{\pm 1/2} = -3A\left(1+\frac{\eta^2}{3}\right)^{1/2}$$
$$E_{\pm 3/2} = +3A\left(1+\frac{\eta^2}{3}\right)^{1/2} \qquad (37)$$

Equation (37) clearly demonstrates that the mixing of the magnetic dipole states does not remove the m- degeneracy of the energy level. Again, only a single frequency is observed for I = 3/2.

$$w\left(\pm 3/2 \rightarrow +1/2\right) = \frac{e^2qQ}{2h}\left(1+\frac{\eta^2}{3}\right)^{1/2} \qquad (38)$$

In a similar manner the secular equations for I = 5/2, 7/2 and 9/2 may be derived. They are tabulated in Table I.

The equations tabulated in Table I are not readily solvable with the exception I = 3/2. A numerical approach is generally used to solve these secular equations[5,26,2,43]. Table II tabulates the absorption frequencies in terms of η, for $\eta \leq 0.25$, where a power series expansion in η may be used.

From the ratio of the measured absorption frequencies it is possible to obtain both η and e^2Qq for nuclei with half integral spins except for I = 3/2. For I = 3/2, Zeeman splitting of the quadrupole frequencies must be studied in order to obtain η and e^2Qq independently.

It was pointed out in the last paragraph that, for I = 3/2, both η and e^2Qq can be independently determined from the ratio of measured absorption frequencies. Cohen[2] has tabulated the eigenvalues

TABLE I

Secular equations for nuclei
with half integral spin

I	Secular Equation	Units of Energy
3/2	$\varepsilon^2 - 3(3+\eta^2) = 0$	$\varepsilon = E/A$
5/2	$\varepsilon^2 - 7(3+\eta^2)\varepsilon - 2(1-\eta^2) = 0$	$\varepsilon = E/2A$
7/2	$\varepsilon^4 - 14(3+\eta^2)\varepsilon^2 - 64(1-\eta^2)\varepsilon + 35(3+\eta^2) = 0$	$\varepsilon = E/3A$
9/2	$\varepsilon^5 - 11(3+\eta^2)\varepsilon^3 - 44(1-\eta^2)\varepsilon^2 + \frac{44}{3}(3+\eta^2)^2\varepsilon + 48(3+\eta^2)(1-\eta^2) = 0$	$\varepsilon = E/6A$

TABLE II

Formulas for the Nuclear Quadrupole Resonance Frequencies[2]

$I = 3/2$	$w = \frac{e^2Qq}{2h}\,(1 + \eta 2/3)^{1/2}$
$I = 5/2$	$w_1 = \frac{3}{20}\,(\frac{e^2Qq}{h})\,(1 + 0.0\,26\,\eta^2 - 0.634\,\eta^4)$
	$w_2 = \frac{6}{20}\,(\frac{e^2Qq}{h})\,(1 + 0.2037\,\eta^2 + 0.162\,\eta^4)$
$I = 7/2$	$w_1 = \frac{1}{14}\,(\frac{e^2Qq}{h})\,(1 + 50.865\,\eta^2 - 101.29\,\eta^4)$
	$w_3 = \frac{3}{14}\,(\frac{e^2Qq}{h})\,(1 - 2.8014\,\eta^2 - 0.5278\,\eta^4)$
	$w_2 = \frac{2}{14}\,(\frac{e^2Qq}{h})\,(1 - 15.867\,\eta^2 + 52.052\,\eta^4)$
$I = 9/2$	$w_1 = \frac{1}{24}\,(\frac{e^2Qq}{h})\,(1 + 9.0333\,\eta^2 - 45.691\,\eta^4)$
	$w_2 = \frac{2}{24}\,(\frac{e^2Qq}{h})\,(1 - 1.3381\,\eta^2 + 11.724\,\eta^4)$
	$w_3 = \frac{3}{24}\,(\frac{e^2Qq}{h})\,(1 - 0.1857\,\eta^2 - 0.1233\,\eta^4)$
	$w_4 = \frac{4}{24}\,(\frac{e^2Qq}{h})\,(1 - 0.0809\,\eta^2 - 0.0043\,\eta^4)$

for the equations listed in Table I for values of η from 0 to 1 at intervals of 0.1. Using these eigenvalues one can plot the calculated frequency ratios vs η for the allowed transitions. From the intercepts of these curves with horizontal lines constructed of the observed frequency ratios, one obtains the value of η. Since a single value of η gives rise to a unique set of frequency ratios, the measure frequency ratios should intercept the calculated curves in a vertical line. Fig. 2 shows an enlarged section of such a plot. Table III contains calculated frequency ratios for transitions of interest in this work.

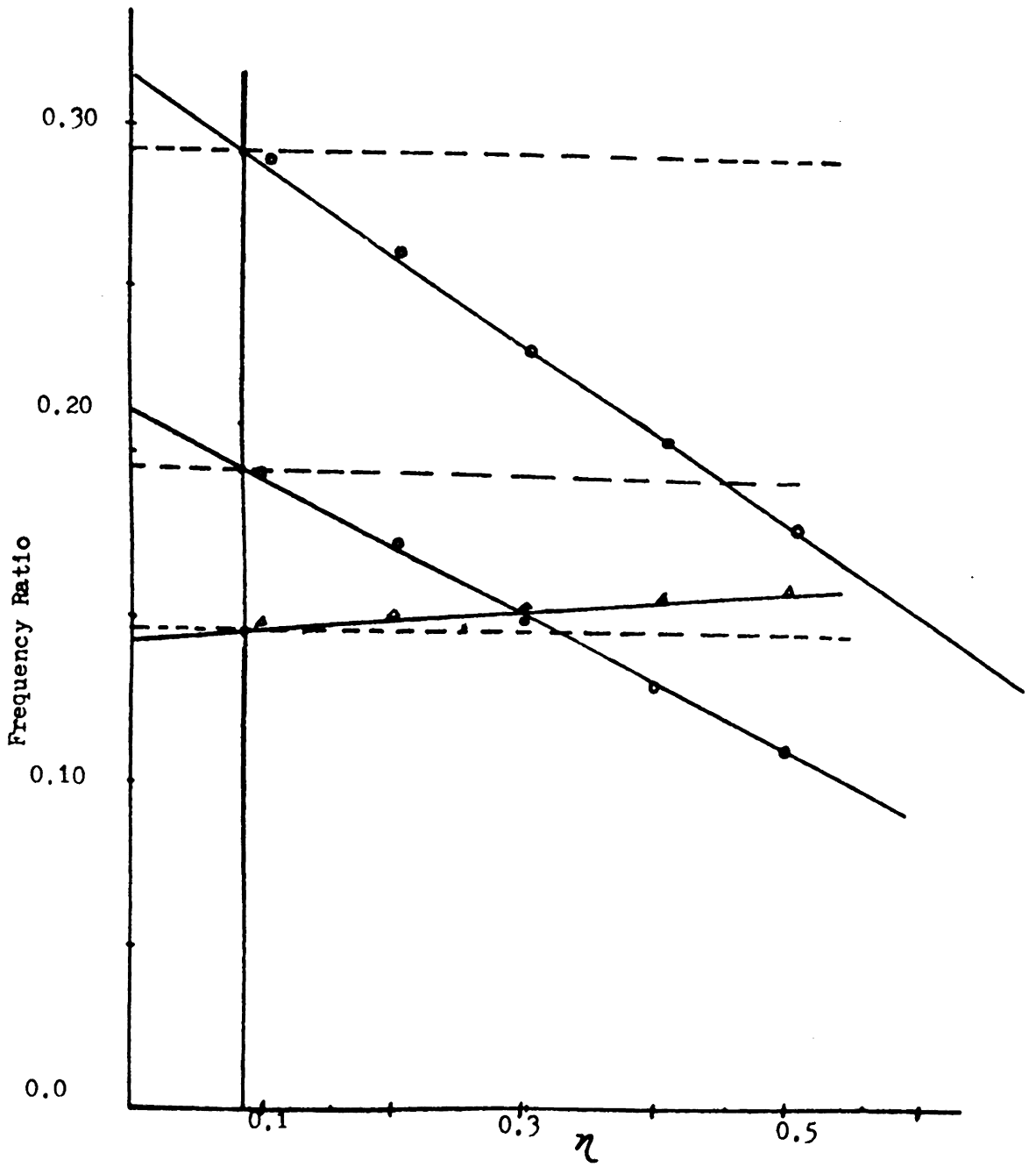

Figure 2

Frequency Ratio vs Asymmetry Parameter

TABLE III

Calculated Frequency Ratio
for I = 7/2

η	$\frac{7/2-5/2}{3/2-1/2}$	$\frac{7/2-5/2}{5/2-3/2}$	$\frac{5/2-3/2}{3/2-1/2}$
0.1	2.89388	1.50676	1.92059
0.2	2.63218	1.52453	1.72655
0.3	2.31877	1.54725	1.49863
0.4	2.02199	1.56812	1.28943
0.5	1.76623	1.58098	1.11716

B. Interpretation of Nuclear Quadrupole Coupling Data

A variety of techniques have been considered for the interpretation of NQR data[7,12,27]. Two methods, the Townes-Dailey approach and a semiquantitative quantum mechanical calculation will be reviewed as they will be refered to in later discussions.

The fundamental quantities determined by nuclear quadrupole resonance measurements are e^2Qq and η. The nuclear quadrupole coupling constant, e^2Qq, is the product of a nuclear property, Q, and a molecular property, q. Since the nuclear quadrupole moment, Q, is a constant for a given nucleus and in most cases is known, the molecular EFG tensor component, q, can be determined from the measured nuclear quadrupole coupling constant. On the other hand, the quantity q could be estimated if the charge distribution over the molecule were known. Due to the non-availability of accurate wave functions q has been rigorously calculated for only a few simple molecules[11,13].

1.) Townes-Dailey Empirical Approach

Townes and Dailey[53] have proposed that the value for eq in a molecule can be expressed in terms of the analogous atomic component, $(eq)_{atm}$. They defined $(eq)_{atm}$ as the electric field gradient tensor component due to an electron in the lowest p-state outside the inner closed shells of the free atom. The relationship between these two quantities is

$$(eq)_{mol} = f\,(eq)_{atm} \tag{39}$$

where f is a factor that depends on the electronic structure of the molecule and is refered to as the p-electron defect. Since Q is a constant for a given nucleus and is independent on the electronic

charge distribution in the molecule, we can write

$$(e^2qQ)_{mol} = f\,(e^2qQ)_{atm} \tag{40}$$

where $(e^2Qq)_{mol}$, and $(e^2Qq)_{atm}$, are the experimentally determined coupling constants for the molecule and the free atom respectively. The free atom nuclear coupling constant can be determined from hyperfine splittings in atomic beam spectra[27].

If f can be written in terms of bonding parameters, information relating to the electronic distribution within the molecule will be available from the experimentally determined molecular coupling constant. For a terminally bonded atom f may be written[7]

$$f = -(1 - s + d - i - \pi) \tag{41}$$

where s and d are the fractions of s- and d-hybridization associated with σ-bonding, i is the fraction of ionic character and π is the fraction of π-bond or multiple bond character. If one can reasonably estimate or experimentally determine some of these parameters, NQR data can be used to obtain the other. Except for transition elements contributions due to d-hybridization can be ignored. Table IV lists experimental values for the "p-electron defect" for several diatomic halogens.

For a homonuclear diatomic molecule, one would expect the hybridization, π-bond character and ionic character would be equal in each atom, the f-value should therefore by unity or very close to unity. This is true for both Br_2 and Cl_2 with f-values of 1.00 and 0.99 respectively. For a hetronuclear diatomic molecule, hybridization,

TABLE IV

Quadrupole Coupling Constants[29] and -f Values for Diatomic Halogen Molecules

Compounds	Nucleus	(e^2Qq)gas MHz	-f	(e^2Qq)crys MHz	-f
ClF	^{35}Cl	146.0	1.33	144.0	1.29
Cl_2	^{35}Cl	--	--	108.50	0.99
ClBr	^{35}Cl	103.6	0.95	--	--
	^{79}Br	876.8	1.14	--	--
ClI	^{35}Cl	82.5	0.75	74.4	0.68
	^{127}I	293.0	1.28	305.7	1.83
BrF	^{79}Br	108.9	1.44	--	--
Br_2	^{79}Br	--	--	765.85	1.00
I_2	^{127}I	--	--	215.6	0.94

π-bond character and ionic character should no longer be equal since the electronegativity difference between the atoms will cause an unbalance in the electron distribution and the resulting f-values should deviate from unity. This is observed for ClI which has f = 0.68 and f = 1.33 for the Cl and I atoms respectively. This has been explained[54] as resulting from a decrease of the p-electron defect on the Cl atoms and an increase of the p-electron defect on the I atoms, i.e. a partial Cl^-I^+ structure. Townes and Dailey have also postulated that for any terminally bonded halogen that is more electronegative than the atom to which it is bonded by 0.25 units, one should allow for 15% s-hybridization. For electronegativity differences of less than 0.25 units no hybridization is allowed. Using this concept, along with quadrupole coupling data, the ionic character of a bond that is reasonably well not expected to exhibit any π-bonding can be found from the relation

$$(e^2qQ)_{mole} = (1-i-s)\ (e^2Qq)_{atm} \qquad (42)$$

Table V lists typical NQR data for some diatomic molecules and the resulting ionic character calculated from this data.

The relationship between the ionic character as calculated from equation (42) and the electronegativity difference between the elements involved in the bond being considered is shown in Fig. 3. Also included in this figure are electronegativity curves due to Gordy[12] and to Pauling[38]. Gordy considered s-hybridization to be zero in calculating ionic character from NQR data. Pauling used the empirical relation

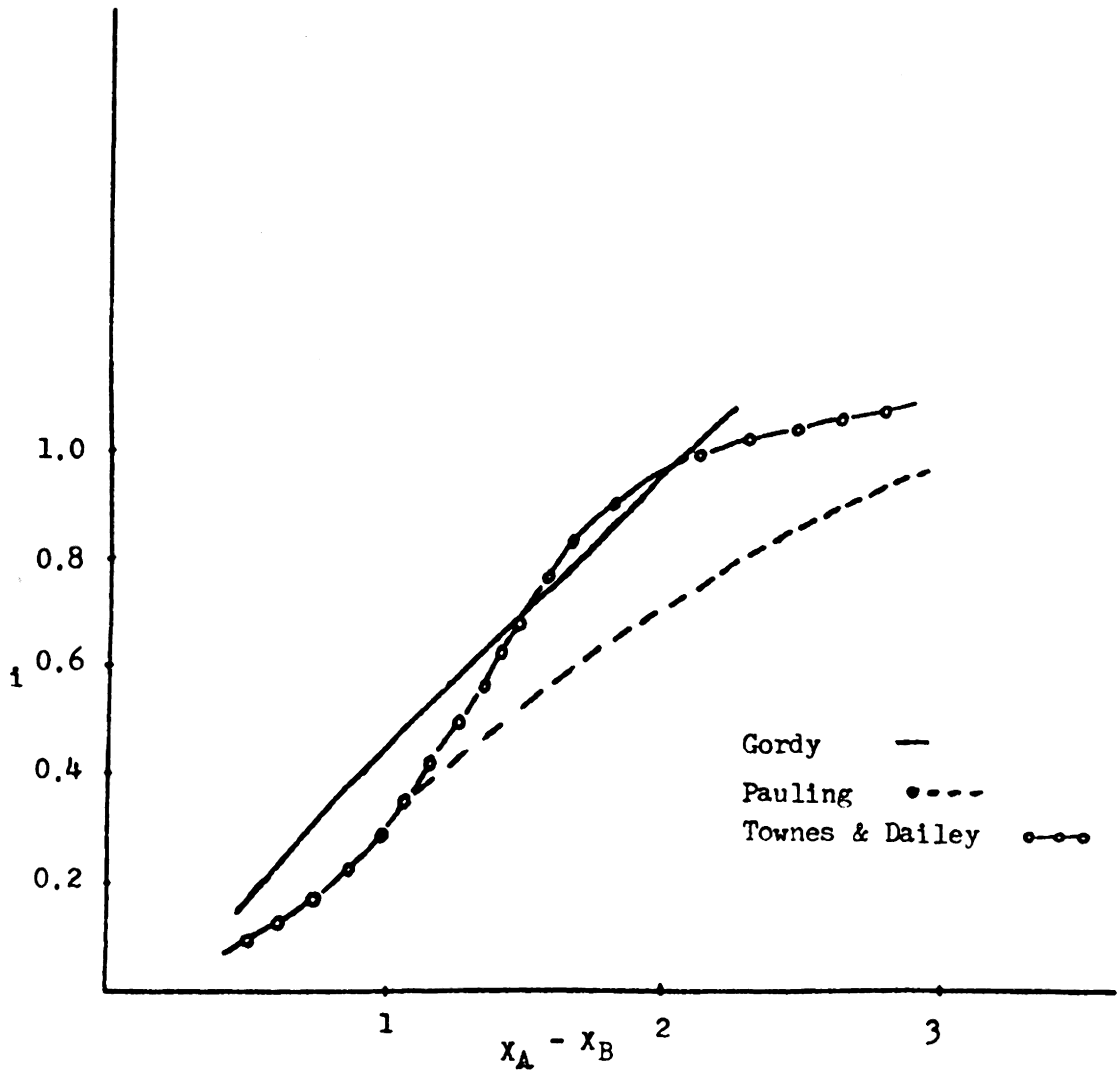

FIGURE 3

Electronegativity Difference vs Ionic Character as Determined by Different Investigators

TABLE V

Ionic Character of Diatomic Halides
Obtained from Nuclear Quadrupole Resonance Data[a]

Molecule	e^2Qq (MHa)	Ionicity assuming no s-hybrid (Gordy)	s-hybrid assumed	ionicity calc. (Townes & Dailey)	electro-negativity difference
^{35}Cl (atm)	109.74	--	--	--	--
BrCl	103.6	0.05	0.0	0.056	0.20
ICl	82.5	0.248	0.15	0.115	0.50
FCl	146.0	0.259	0.0	0.259	0.75
TlCl	15.8	0.856	0.15	0.831	1.75
KCl	0.04	1.00	0.15	1.000	2.35
RbCl	0.774	0.993	0.15	0.992	2.35
CsCl	3	0.973	0.15	0.968	2.45
^{79}Br (atm)	769.76	--	--	--	--
BrCl	876.8	0.110	0.0	0.110	0.20
FBr	1089.0	0.329	0.0	0.329	0.95
LiBr	37.2	0.952	0.15	0.944	1.95
NaBr	58	0.925	0.15	0.911	2.05
KBr	10.244	0.987	0.15	0.985	2.15
DBr	533	0.308	0.15	0.186	0.75

[a]Reference 29.

$$i = 1 - \exp \frac{1}{4}(X_A - X_B)^2 \qquad (43)$$

where X_A and X_B are the electronegativity values for atoms A and B forming the bond. It is clear that the differences between the two NQR data approaches are small. A major difference exists between the curves derived from NQR data and the curve due to Pauling. This is because the ionic character as calculated from electronegativity values alone neglects such effects as polarization and hybridization. On the other hand, quadrupole coupling constants are related to the total electronic structure of the molecule. Thus ionic character calculated from NQR data are probably more accurate.

The amount of π -bonding involved in a compound increases the p-electron defect, thereby affecting the quadrupole coupling constant by decreasing its magnitude. To account for this, Equation (42) can be rewritten as

$$(e^2Qq)_{mol} = (1-i-s-\pi)\,(e^2Qq)_{atm} \qquad (44)$$

The p-electron defect has now been related to the quadrupole coupling constant. Since it is directly related to the population of electrons in the p-orbitals we can next relate the quadrupole coupling constant directly to the p-orbital populations, N_x, N_y and N_z. For any atom irrespective of its mode of bonding it has been shown that[20]

$$e^2Qq_{xx} = -\left(\frac{N_z + N_y}{2} - N_x\right)(e^2Qq)_{at} \qquad (45)$$

$$e^2Qq_{yy} = -\left(\frac{N_x + N_z}{2} - N_y\right)(e^2Qq)_{at} \qquad (46)$$

$$e^2Qq_{zz} = -\left(\frac{N_y+N_x}{2} - N_z\right)(e^2Qq)_{at} \tag{47}$$

From these relations it is found that

$$\eta = \frac{3(N_y-N_x)}{N_x+N_y-2N_z} \tag{48}$$

For transition metal elements where d-electrons are involved in bonding the populations of the d-orbitals can be related to the quadrupole coupling constant by

$$(e^2Qq)_{mol} = \left[(e^2Qq)_{at}\left(N_{d_{z^2}} + \frac{N_{d_{xz}}+N_{d_{yz}}}{2} - N_{d_{xz}} - N_{d_{x^2y_z}}\right)\right] \tag{49}$$

2). Semiquantitative Quantum Mechanical Evaluation of Electrostatic Field Gradient Tensor Components in a Molecule

In order to accurately calculate the electrostatic field gradient tensor components in molecules, one must have the exact wavefunctions. At present exact wavefunctions for complex molecules are not available. It is possible however to make some reasonable and useful estimates of EFG tensor components by using a molecular model based on conventional hybridization schemes. The method employed is to relate the contribution of electrons in a particular hybrid orbital to that of electrons in pure atomic orbitals where the latter are represented by either hydrogen like or Slater type orbitals. The contribution of a particular hybrid orbital, is then obtained by use of the conventional average value expression

$$q_{gg'} = \int_0^{\infty}\int_0^{\pi}\int_0^{2\pi} \psi_i^* (q_{gg'})_{op} \psi_i \, r^2 \sin\theta \, dr \, d\theta \, d\phi \qquad (50)$$

where gg' is a pair of cartesian coordinates and $(q_{gg'})_{op}$ is the appropriate EFG tensor component operator (Table VI). It is noted that these components are products of angular and radial functions, the latter of which are generally common for all atomic orbitals involved in the calculation. S-orbitals will not contribute to the EFG tensor because of their spherical symmetry. By using hydrogen-like wavefunctions, the radial part is given by[20]

$$\left\langle \frac{1}{r^3} \right\rangle_{av} = \frac{2Z'}{n^3 a_o^3 l(l+1)(2l+1)} \qquad (51)$$

where n is the principal quantum number, l is the orbital quantum number, Z' is the effective atomic number and a_o is the Bohr radius. By using the rules given by Kauzmann[20] for calculation of screening constants the effective atomic number of any atom can be estimated. The EFG tensor components for a single electron in the bonding atomic orbitals of a Cu atom as calculated by using equations (50), (51) are tabulated in Table VII. Since the Cu atom will be discussed at considerable length later it will be used as an example to illustrate the method of calculation. As a start one employs any available bonding information to construct a suitable model. Consider the σ-bonding orbitals of the Cu atom to be 4 sp^3-hybrid orbitals of the general form:

TABLE VI

Operators for EFG
Tensor Components

$q_{xx} = (\frac{e}{r^3})(3\sin^2\theta\cos^2\phi - 1)$	$q_{yy} = (\frac{e}{r^3})(3\sin^2\theta\sin^2\phi - 1)$
$q_{xy} = (\frac{e}{r^3})(3\sin^2\theta\cos\phi\sin\phi)$	$q_{yz} = (\frac{e}{r^3})(3\sin\theta\cos\theta\sin\phi)$
$q_{xz} = (\frac{e}{r^3})(3\sin\theta\cos\theta\cos\phi)$	$q_{zz} = (\frac{e}{r^3})(3\cos^2\theta - 1)$

TABLE VII

EFG Tensor Components for Cu

Atomic Orbitals	Contribution of a single electron in a single atomic orbital EFG tensor component X 10^{-14} esu cm^{-3}		
	q_{xx}	q_{yy}	q_{zz}
$4p_x$	-6.84	3.42	3.42
$4p_y$	3.42	-6.84	3.42
$4p_z$	3.42	3.42	-6.84
$3d_{z^2}$	1.16	1.16	-2.32
$3d_{x^2-y^2}$	-1.16	-1.16	2.32
$3d_{xy}$	-1.16	-1.16	2.32
$3d_{xz}$	-1.16	2.32	-1.16
$3d_{yz}$	2.32	-1.16	-1.16

$$\begin{aligned}
\Psi_1 &= a_1 s + b_1 P_x + c_1 P_y + d_1 P_z \\
\Psi_2 &= a_2 s + b_2 P_x + c_2 P_y + d_2 P_z \\
\Psi_3 &= a_3 s + b_3 P_x + c_3 P_y + d_3 P_z \\
\Psi_4 &= a_4 s + b_4 P_x + c_4 P_y + d_4 P_z
\end{aligned} \tag{52}$$

These hybrid orbitals are oriented relative to an arbitrary cartesian coordinate system which may be chosen to coincide with the crystal axis system or may be related in some symmetrical way to the bond directions. The nucleus (Cu atom) in question is located at the origin. If the directions of the hybrid orbitals do not coincide with bond directions one can rewrite the hybrid orbitals in the form,

$$\begin{aligned}
\Psi_1 &= a_1 s + b_1 \mathrm{Cos}\,\alpha_1 P_x + C_1 \mathrm{Cos}\,\beta_1 P_y + d_1 \mathrm{Cos}\,\gamma_1 P_z \\
\Psi_2 &= a_2 s + b_2 \mathrm{Cos}\,\alpha_2 P_x + C_2 \mathrm{Cos}\,\beta_2 P_y + d_2 \mathrm{Cos}\,\gamma_2 P_z \\
\Psi_3 &= a_3 s + b_3 \mathrm{Cos}\,\alpha_3 P_x + C_3 \mathrm{Cos}\,\beta_3 P_y + d_3 \mathrm{Cos}\,\gamma_3 P_z \\
\Psi_4 &= a_4 s + b_4 \mathrm{Cos}\,\alpha_4 P_x + C_4 \mathrm{Cos}\,\beta_4 P_y + d_4 \mathrm{Cos}\,\gamma_4 P_z
\end{aligned} \tag{53}$$

where α_i, β_i, γ_i $(i = 1,2,3,4)$ are the angles relating the directions of the bonds to the cartesian, axis system. Since the hybrid orbitals will be normalized there are eight relations

$$a_i^2 + b_i^2 \mathrm{Cos}\,\alpha_i^2 + C_i^2 \mathrm{Cos}\,\beta_i^2 + d_i^2 \mathrm{Cos}\,\gamma_i^2 = 1$$

$$\Sigma_i a_i^2 = 1$$

$$\Sigma_i\, b^2 \cos\alpha_i^2 = 1 \qquad (54)$$

$$\Sigma_i\, c^2 \cos\beta_i^2 = 1$$

$$\Sigma_i\, d^2 \cos\gamma_i^2 = 1$$

These eight equations can be solved simultaneously to yield value for the constants. The final form of the hybrid orbitals then becomes

$$\begin{aligned}
\psi'_1 &= a_1' s + b_1' P_x + c_1' P_y + d_1' P_z \\
\psi'_2 &= a_2' s + b_2' P_x + c_2' P_y + d_2' P_z \\
\psi'_3 &= a_3' s + b_3' P_x + c_3' P_y + d_3' P_z \\
\psi'_4 &= a_4' s + b_4' P_x + c_4' P_y + d_4' P_z
\end{aligned} \qquad (55)$$

These functions are used to calculate the EFG tensor components by using equation (50) along with the appropriate EFG operators. The EFG tensor components due to a single electron in each hybrid orbital is thus calculated. Since, in most cases, an atom will contribute either more or less than one electron to a bond with other atoms, we are confronted with the problem of assigning the number of electrons present in a given hybrid orbital. This is done with the aid of auxillary information such as the ionicity of the bond as calculated from electronegativity differences and the possibility of the existance π-character. Finally, the sum of the contributions of each hybrid orbital to the EFG tensor components is determined and the results compared to experimental values.

LITERATURE REVIEW

A. Bis(tetracarbonylcobalt)tin Derivatives

The insertion of tin(II) halides into cobalt carbonyl to form a metal-metal covalent bond was first reported by Heiber[23] in 1957. Later, in a series of papers, Graham[16,18,19,30-37,45,52] extended this investigation to include all elements in the fourth group with a number of transition metal carbonyls such as Mn, W, and Rh. Most of the compounds reported were prepared by conventional halide displacement or by direct reaction of MX_4 with metal carbonyls. They are crystalline materials, stable under a nitrogen atmosphere but decompose on exposure to air.

Infrared studies on a number of bis(tetracarbonylcobalt) derivatives of tin and germanium revealed that the C≡O stretching frequency tends to shift to higher values as the electronegativity of the halogen substituents on the metal atom increases (Table VIII). Furthermore, if one plots the frequencies of the A_1 or A_1' CO stretching modes against the Pauling[38] electronegativity of the halogen substituent a linear relationship is obtained, Figure 4 illustrates this for the germanium compounds. These trends are true not only for bis(tetracarbonylcobalt) compounds of germanium or tin, but also for mono and tris(tetracarbonylcobalt) derivatives of all elements in fourth group except carbon. These trends have been explained in terms of substituent effects on π-bonding in the molecules. Figure 5 represents schematically the π-interactions between the metal atoms and the ligands. There are two electrophilic sites, Ge and CO, competing for the electron density

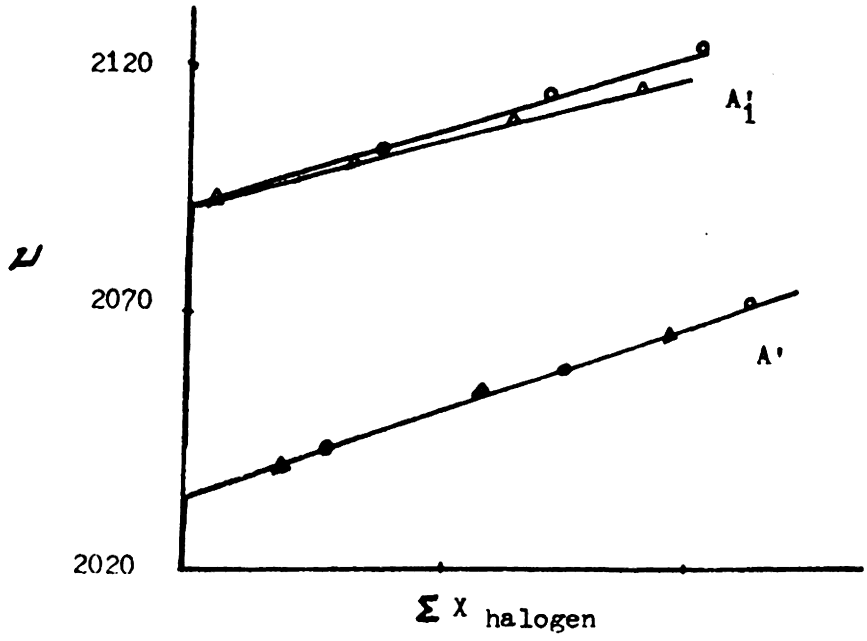

FIGURE 4

Effect of Halogen Substitutents on the Carbonyl Stretching Frequencies in $X_nR_{3-n}GeCo(CO)_4$

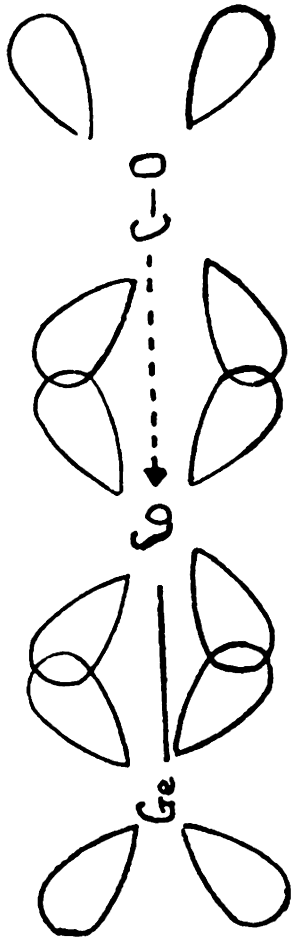

Figure 5

Schematic Representation of π-Interaction
Between Ge-Co and Co-CO Groups

TABLE VIII

Infrared Spectra of Bis(tetracarbonylcobolt) derivatives[a]

Compounds with C_{2v} Symmetry	A_1	B_1	$2A_1$ +	$2B_1$ +	B_2		
$Cl_2Ge[Co(CO)_4]_2$	2117	2100	2058	2054	2044	2026	2016
$I_2Ge[Co(CO)_4]_2$	2113	2096	2054	2051	2042	2025	2013
$(CH_3)_2Ge[Co(CO)_4]_2$	2098	2081	2033	2027	2019	2006	1997
$Cl_2Sn[Co(CO)_4]_2$	2114	2097	2056	2052	2040	2023	2016
$Br_2Sn[Co(CO)_4]_2$	2113	2096	2055	2050	2040	2036	2016
$I_2Sn[Co(CO)_4]_2$	2110	2093	2053	2048	2037	2021	2012
$(CH_3)_2Sn[Co(CO)_4]_2$	2095	2078	2031	2024	2013	2002	1992
$\phi_2Sn[Co(CO)_4]_2$	2095	2080	2033	2039	2018	2009	1995
$(CH_2{=}CH)_2Sn[Co(CO)_4]_2$	2097	2080	2037	2028	2018	2009	1998

TABLE VIII (con't)

Compounds with C_s Symmetry	A_1'	A"	3A' + 3A"					
$I(CH_3)Ge[Co(CO)_4]_2$	2106	2089	2046	2040	2030	2024	2014	2000
$Cl(CH_3)Sn[Co(CO)_4]_2$	2104	2088	2044	2038	2022	2017	2005	1996
$Cl\phi Sn[Co(CO)_4]_2$	2105	2088	2045	2039	2030	2021	2014	1999
$Cl(n\text{-}C_4H_9)Sn[Co(CO)_4]_2$	2103	2086	2044	2037	2024	2018	2007	1996
$Cl(CH_2{=}CH)Sn[Co(CO)_4]_2$	2101	2088	2046	2040	2029	2022	2017	2000

[a]Reference 36

in the filled cobalt 3d-π-orbitals. Any increase in π-bonding of either the Ge or CO must occur at the expense of the other. Suppose the π-bonding between germanium and cobalt increases, the π-bonding between carbon monoxide and the cobalt atom must accordingly decrease. Consequently, the carbon monoxide will experience an increase in bond order and hence in the magnitude of the C≡O stretching frequencies. The inductive effect of the substituents on the germanium atom will increase or decrease the electron affinity of the empty 4d-germanium orbitals. For a highly electronegative substituent such as chlorine, the electron affinity of the empty 4d-π orbitals increases. This in turn provides the germanium atom with a greater ability to accept electrons from the cobalt atom to form a stronger π-bond. This produces the effects cited above. Graham also observed from the infrared studies that there is a considerable coupling of the vibrational modes of the two $Co(CO)_4$ groups across either a germanium or a tin atom in the bis-compounds. Such a coupling can be simply explained by symmetry considerations. For molecules of C_{2v} or C_s symmetry, group theory predicts seven infrared active bands ($3A_1 + 3B_1 + B_2$) for the C_{2v} case and eight infrared active bands ($4A_1 + 4A''$) for the C_s case. However, on the basis of the "local symmetry" of the two equivalent $Co(CO)_4$ groups, one would expect only three or four frequencies that are infrared active if one assumes there is no coupling between two equivalent $Co(CO)_4$ groups.

The fact that seven or eight absorption bands were observed (Figure 6, 7) is a clear indication of coupling between the vibrational modes of the two $Co(CO)_4$ groups across the germanium or tin atom.

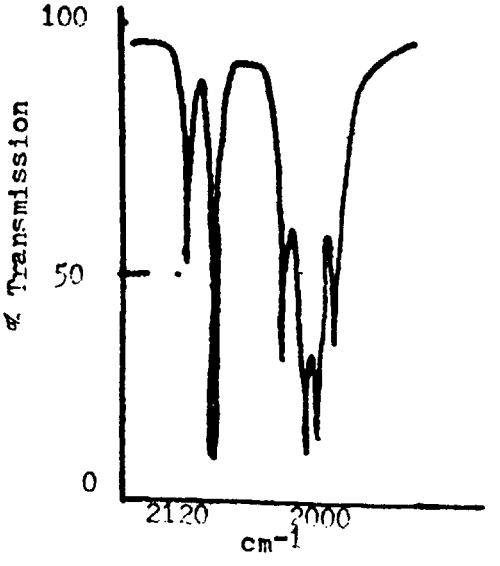

FIGURE 6

Infrared Spectrum of $\phi ClSn\ Co(CO)_4$ - C_s Type

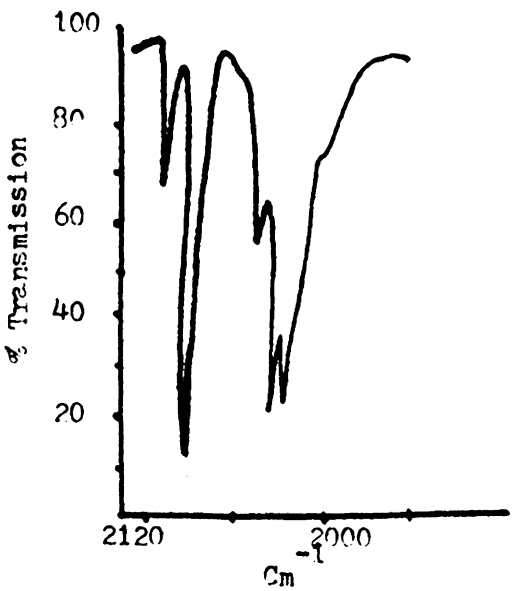

FIGURE 7

Infrared Spectrum of $\phi_2 Sn\ Co(CO)_4$ $_2$ - C_{2v} Type

From infrared intensity measurements it was found that the intensity of the A_1 mode (Figure 8), in which the C≡O dipoles of the two $Co(CO)_4$ tend to oppose each other, was, in general, weak and tended to increase as the Co-M-Co angle decreased. The intensity of the B_1 mode (Figure 9) where the dipoles tend to reinforce one another increases with increasing Co-M-Co angle. If one assumes collinearity of the dipoles[17] on the cobalt atom and the M-Co bond then a simple geometrical relation can be formulated,

$$\frac{A_{A1}}{A_{B1}} = \text{Cot } (\frac{\theta}{2})^2 \qquad (51)$$

where A is the absorbance of the indicated band and θ is the Co-M-Co angle. The observed absorbance ratios and the Co-M-Co angles for bis(tetracarbonylcobalt) derivatives of germanium and tin are given in Table IX. It is interesting to observe, the "bond angle" tends to increase as the electronegativity of the substituents increase. One must not take the "bond angle" literally. The trends, however, are as would be expected on the basis of Bent's rule[1], i.e., that electronegative substituents tend to free the s-character of the tin or germanium atom σ-bonding orbitals for use in the metal-metal bonds, with a resulting increase in the metal-metal bond angle. NMR studies of chemical shifts[9,17,10] and proton-tin coupling constants in methyl tin derivatives suggest that this is indeed the case. Table X lists the NMR results.

Kaesz[10], et.al. suggested that the coupling of the spins of the adjacent nuclei by means of bonding electrons is expected to be propor-

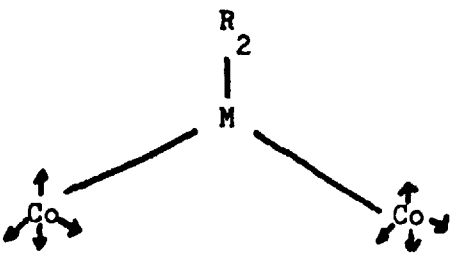

FIGURE 8

A_1 mode

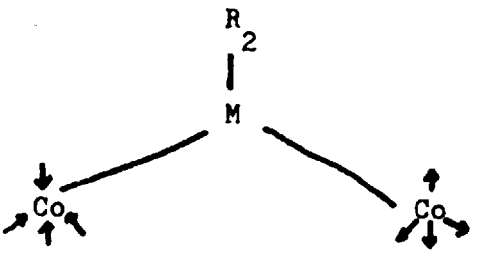

FIGURE 9

B_1 mode

TABLE IX

The observed absorbance ratios and the Co-M-Co angles in Bis(tetracarbonyl cobalt) derivatives of Sn and Ge compounds

Compounds	A_{A_1}/A_{B_1}	Cot $\theta/2$	θ
$Cl_2Ge[Co(CO)_4]_2$	1.04×10^{-2}	0.102	169°40'
$I_2Ge[Co(CO)_4]_2$	014.1	0.64	115.15'
$(CH_3)_2Ge[Co(CO)_4]_2$	0.38	0.618	117.28'
$Cl_2Sn[Co(CO)_4]_2$	1.01×10^{-2}	0.1005	169°28'
$Br_2Sn[Co(CO)_4]_2$	1.03×10^{-2}	0.1015	169°38'
$I_2Sn[Co(CO)_4]_2$	0.365	0.604	116°16'
$(CH_3)_2Sn[Co(CO)_4]_2$	0.370	0.608	116°36'
$(\emptyset)_2Sn[Co(CO)_4]_2$	0.515	0.718	105°22'
$(CH_2{=}CH)_2Sn[Co(CO)_4]_2$	0.460	0.678	110°16'
$I(CH_3)Ge[Co(CO)_4]_2$	0.290	0.538	122°34'
$Cl(CH_3)Sn[Co(CO)_4]_2$	0.300	0.548	123°28'
$Cl\emptyset Sn[Co(CO)_4]_2$	0.330	0.574	120°42'
$Cl(Cl\text{-}C_4H_9)Sn[Co(CO)_4]_2$	0.330	0.574	120°42'
$Cl(CH_2{=}CH)Sn[Co(CO)_4]_2$	0.430	0.656	112°36'

TABLE X

NMR Spectra[a]

Compounds	τ	$J(^{117}Sn\text{-}CH_3)$	$J(^{119}Sn\text{-}CH_3)$
$(CH_3)_3Sn\ Co(CO)_4$	9.37	50.6	52.6
$(CH_3)_2Sn[Co(CO)_4]_2$	8.88	43.6	45.7
$CH_3Cl\ Sn[Co(CO)_4]_2$	8.48	42.2	--
$CH_3Sn[Co(CO)_4]_3$[b]	8.98	33.0	--

[a] in $CDCl_3$ solution

[b] Reference 33

tional to the densities of the bonding electrons at the respective nuclei. Thus, the coupling of the nuclei will be greater when there is a larger amount of s-character in the overlapping hybrid atomic orbitals that form the bond between them. For the proton-tin system, the interaction or coupling takes place between two bonds, C-H and Sn-C. Since the variation is small between $J(C^{13}H_3)$ = 129.2 cps for $(CH_3)_2SnMn(CO)_5$[35] and $J(C^{13}H_3)$ = 128.0 cps[36] for $(CH_3)_4Sn$, it is reasonable to assume that the hybridization of the carbon atom remains constant. The observed change of the proton-tin coupling constants can then be attributed to the variation of the s-character in the tin s-p hybrid orbitals which are directed toward the methyl groups. The observed decrease in the coupling constants as the number of methyl substituents decreases suggests that the tin σ-orbitals bonded to the cobalt atom is enriched in s-character, in accordance with Bent's rule.

B. Cu(I) thiourea and substituted thiourea complexes

1. Thiourea complexes

Cu(I) thiourea complexes were prepared in the early 1900's by a number of German workers[40,41]. It was proposed by Rathke[40,41] that the bonding in these complexes was through the sulfur atoms with a structure of the form

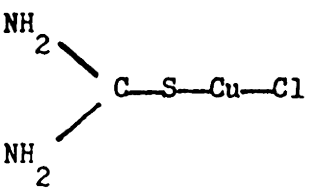

X-ray crystal structure studies have since revealed a[21] number of different types of metal-sulfur bonds in compounds of this type. Typical of this are the observations of the occurance of an electron deficient bond in $Cu(tu)_9(NO_3)_4$ and of sulfur bridging in $Ag(tu)_2Cl$.

Yamaguchi[59] and Irving[50] reached similar conclusion that the complexes are coordinated through the sulfur atom via infrared studies on a number of complexes of thiourea with various metals. Their conclusions were based on the weakening or complete disappearance of the band at 1083 cm^{-1} and the lowering of the frequency of the band at 730 cm^{-1}. Yamaguchi suggested that the weakening of the band at 1083 cm^{-1} was due to the decreasing of C=S stretching frequency and an increasing in N-C-N stretching frequency. The lowering of the frequencies was contributed to the decrease of double bond character of the C=S bonds. Their conclusion was substantiated by subsequent X-ray studies on $Zn(tu)_2Cl_2$,[55] $Cu(tu)_3Cl$,[56] and $Cu(tu)_2Cl$[48,49].

The crystal structures of both the tris and bis(thiourea) Copper(I) chlorides are of interest for subsequent nuclear quadrupole resonance interpretation, and therefore warrant a detail description. Knobler et.al.[21] found that tris(thiourea) Copper(I) chloride crystallizes in the tetragonal system with a = 13.41 A and c = 13.76 A. The structure consists of long spiral chains of $Cu(tu)_3^+$ ions (Figure 10) interspersed with chloride ions. It was found that the copper atom is surrounded by four sulfur atoms, two of which are shared by two copper atoms and serve as links to form the chain structure. The internuclear distances of the Cu-S bonds are 2.13 A, 2.34 A, 2.33 A and 2.42 A. The former two are the Cu-S distances of the unshared sulfur atoms and the

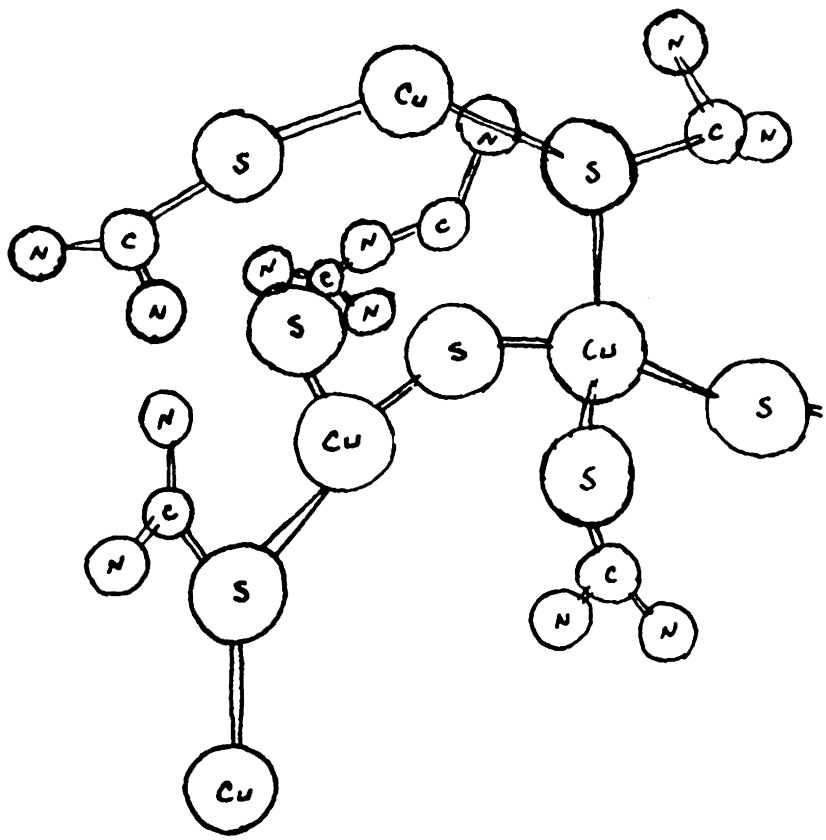

FIGURE 10

View Along the b-Axis Showing the
Chain Type Structure in Tristhiourea Copper(I) Chloride

latter two are for the shared sulfur atoms distances. The configuration of the copper atom is a slightly distorted tetrahedron with S-Cu-S angles varying from 101 degrees to 108 degrees.

Table XI lists the structural parameters of the thiourea ligands in the crystalline complex along with those of uncoordinated thiourea. Three ligands have, at least one C-N bond length that is shorter than the C-N bond length in the uncoordinated thiourea and is closer to the C=N double bond distance of 1.21-1.28 A, while ligand I has two almost equal C-N distances. The short C-N bond lengths were rationalized in terms of resonance structures of the ligand[25]:

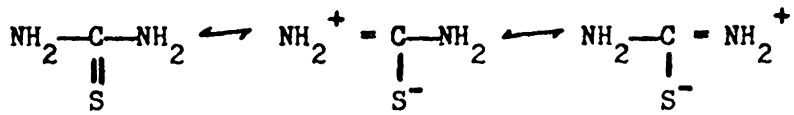

It is not certain what the reason is for the existance of unequal C-N bonds in both ligand II and III which are single coordinated. One suggested explanation was interaction of the anions which causes distortion of the chain. It was further pointed out that all the ligands lie in the same plane within experimental error.

The crystal structure of the bis(thiourea) Copper(I) chloride was reported by Amma et. al.[48,49] Both the geometry and the bonding were somewhat novel for Cu(I) compounds. The Cu atom is located in a near trigonal planar environment surrounded by sulfur atoms from three different thioureas. The sulfur atoms at two of each of the three trigonal positions are shared by different copper atoms to form infinite spiral chains (Figure 11) similar to the tris-compound. Each Cu atom has associated with it a long axial Cu-Cl distance. The bonding

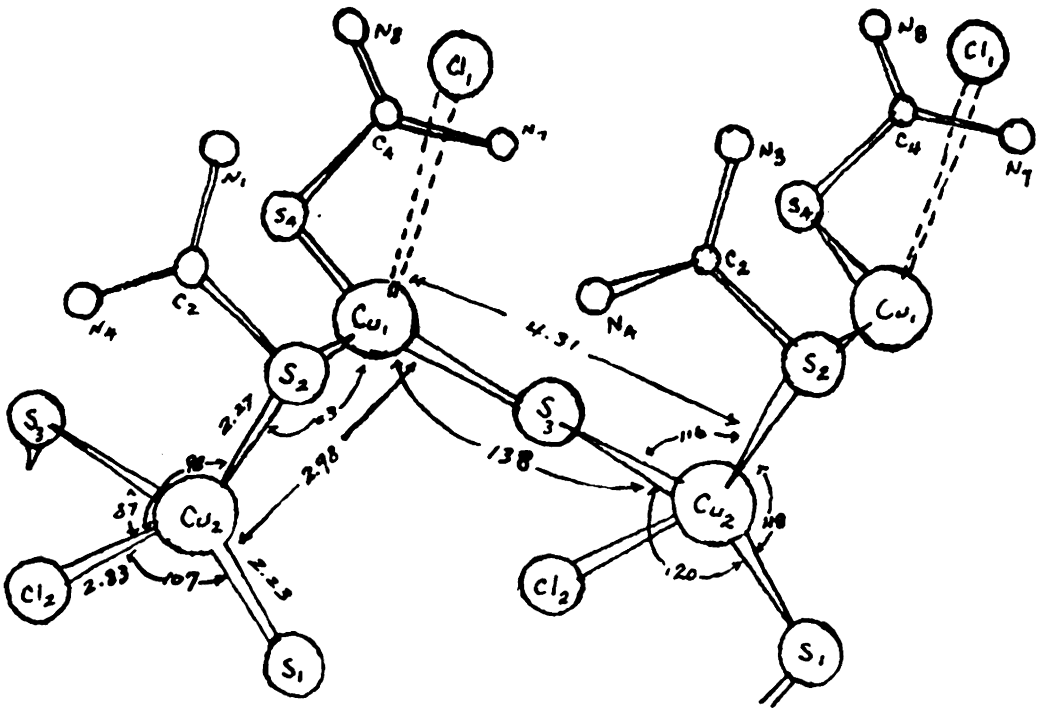

Figure 11

View of the Bis(thiourea) Copper (I) chloride Chain Down the b-axis Showing the Important Distances and Angles

TABLE XI

Bond angles (deg) and lengths (A) in thiourea and tris(thiourea)Copper(I) chloride

	C=S	C-N	C-N'	S-C-N	S-C-N'	N=C=N
Thiourea	1.705	1.313	1.313	122.5	122.5	115.0
I	1.797	1.241	1.290	114.8	114.2	129.9
II	1.820	1.287	1.398	127.4	111.4	121.1
III	1.832	1.458	1.195	109.8	123.8	124.3

between Cu-Cl is considered as ionic. It was pointed out that the Cu-Cu separation alternated between a long and a short distance with an accompaning "broad" and "sharp" Cu-S-Cu bridging angle. The short metal-metal distances with the sharp bridging angle was explained by the formation of a three-center electron pair bridging bond, resulting from the overlap of sp^2 orbitals from each Cu atom and a p-orbital from the s atom (Figure 12). The formation of the "broad" bridging angle and accompanying larger bond lengths was suggested as being due to the overlap of π -bonding orbitals on both the Cu and S atoms.

2. Substituted thiourea Copper(I) complexes

Morgan and Burstall[29] prepared a variety of Copper(I) ethylene thiourea salts. These include:

$Cu(etu)_4NO_3$ --- Colorless prismatic crystals

$Cu_2(etu)_5(NO_3)_2 4H_2O$ --- White, six-sided prismatic

$Cu(etu)_{3\ 2}SO_4$ --- Colorless, three-sided prismatic

$Cu(etu)_3Ac$ --- Colorless, eloagated plate

$Cu(etu)_2Cl$ --- Colorless, rhombic

$Cu(etu)_2O$ --- Floculent, white

etu = ethylene thiourea

The structure of these compounds was considered to involve Cu-S bonding. A limit of four-fold coordination was recognized. In the limit of four coordinated ligands per Cu the Cu will have acquired eight electrons, giving it a krypton structure. Neither crystal structure analysis nor infrared spectroscopic studies been done on any of the ethylene thiourea complexes, except $Cu(etu)_4NO_3$[25].

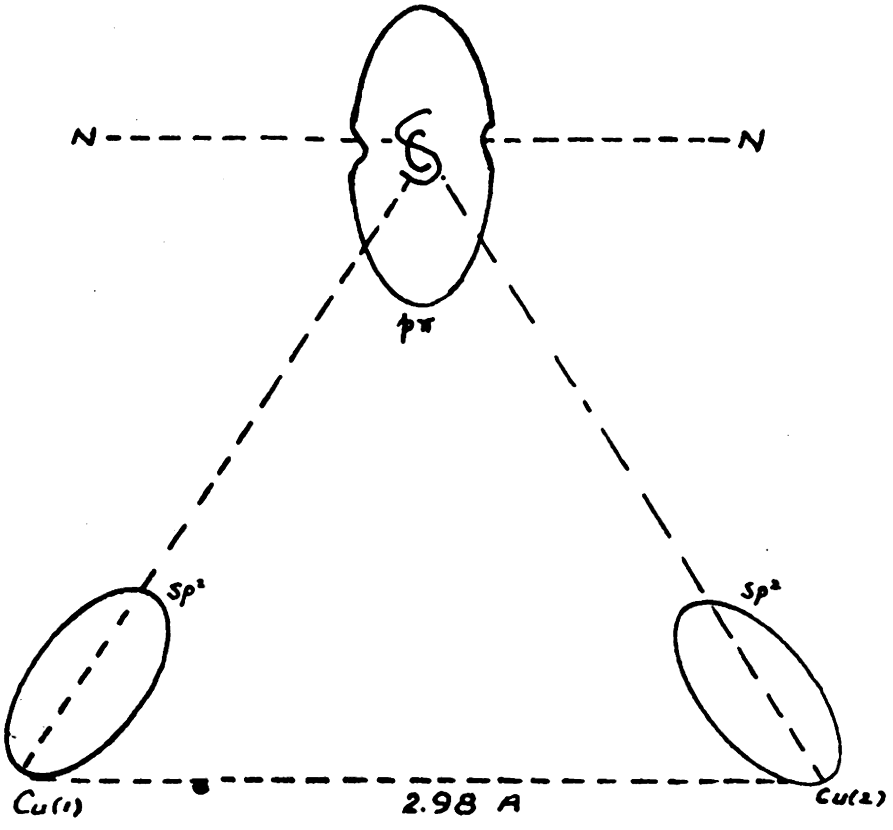

FIGURE 12

View normal to Cu(1)-S(2)-Cu(2) plane of orbitals used to make the three center delocalized electron pair bridge bond.

EXPERIMENTAL

A. Preparatory work

1. Bis(tetracarbonylcobalt)tin Compounds

All of the compounds studied were prepared by the procedure given by Patmore and Graham. All reactions were carried out under a static nitrogen atmosphere and the solid products were sealed in screw cap vials using teflon tape to minimize exposure to air. Table XII lists the physical properties of the compounds prepared along with the results given by Graham. In addition to the use of color and melting points to ascertain the composition of the products the infrared spectra of all three compounds were found to be in complete agreement with those published by Graham.

2. Copper(I) thiourea and substituted thiourea complexes

a. Tris(N,N,'-dimethylthiourea)copper(I)chloride: This compound was prepared by dissolving 5.25g N,N'-dimethylthiourea (Aldrich Chemical Company, Inc., Cat. #D18,870-0) in a minimum amount of methanol and reacting this solution with a solution of 8.55gm $CuCl_2 \cdot 2H_2O$ prepared in a similar manner. The mole ratio of the two components was 4:1. The solution was concentrated by boiling until a yellow precipitate of sulfur formed. This was removed by suction filtration. Further concentration yielded a yellow viscous liquor which on cooling and stirring very slowly formed creamy white crystals. The crystals were filtered by suction, washed with acetone and air dried. The resulting solid was recrystallized with some difficulty and loss from methanol. Table XIV list the C,H,N, elemental analysis for this and other copper compounds.

TABLE XII

Physical properties of
bis(tetracarbonylcobalt)tin compounds

	Color		Melting Point	
	This work	Graham	This work	Graham
$Co(CO)_4)_2\ SnCl_2$	orange-red	orange-red	104	105
$Cl\phi Sn\ Co(CO)_{4\ 2}$	yellow	yellow	128-132	128-131
$\phi_2 Sn\ Co(CO)_{4\ 2}$	yellow-orange	yellow-orange	71-73	71-73

TABLE XIII

Elemental analysis for copper compounds

	Calc.			Found		
	C	H	N	C	H	N
$Cu_2(etu)_6SO_4$	25.62	4.29	19.99	25.53	4.33	19.96
$Cu(etu)_2Br$	20.80	3.50	16.4	21.18	3.64	17.35
$Cu(etu)_2Cl$	25.15	4.22	20.02	24.25	4.03	19.87
$Cu(tu)_2Br$	8.10	2.69	18.70	8.15	2.93	18.00
$Cu(tu)_2NO_3$	8.62	2.87	24.12	8.54	2.96	23.97
$Cu(tu)_2Cl$	9.45	3.52	22.02	9.87	3.63	21.87
$Cu(etu)_2ClO_4$	20.65	4.85	16.10	20.51	4.55	15.88
$Cu(mtu)_4Cl$	20.94	5.21	24.41	20.66	5.11	24.35
$Cu(dmtu)_3Cl$	26.27	5.85	20.43	26.36	6.00	20.26

etu = ethylenethiourea

tu = thiourea

dmtu = dimethylthiourea

mtu = methylthiourea

b. Tetrakis(N-methylthiourea)copper(I)chloride: This compound was prepared by the method described by Urbanik. A solution of 0.36g N-methylthiourea (A.C.C. M8460-7) (0.04 mole) in a minimum amount of methanol was to a solution of 1.71g $CuCl_2 \cdot 2H_2O$ (0.01 mole) in a minimum amount of methanol. The procedure for concentration described in (a) above was followed. Concentration yielded pale-creamy white crystals. These were filtered by suction, washed with methanol and air dried. This complex was insoluble in most common organic solvents, including ethanol, acetone, benzene, carbon tetrachloride, and chloroform. It was also insoluble in water, but was very slightly soluble in methanol. The melting point range of this compound was 145-147.

c. Bis(ethylenethiourea)copper(I)chloride: This compound was prepared by a method suggested by Morgan and Burstall. 0.04 moles of ethylene thiourea (EKC-No. 5950) was in dissolved in 100 ml of water. 0.01 moles of cupric chloride was added to the aqueous ethylenethiourea solution. The solution was concentrated by boiling until crystals began to fomr. The solution was cooled to room temperature filter. The compound was recrystallized from water.

d. Bis(ethylenethiourea)copper(I)bromide: This compound was prepared by the manner described in (c) above with the substitution of $CuBr_2$ for $CuCl_2$.

e. Tetrakis(ethylenethiourea)copper(I)nitrate: This compound was prepared by the manner described in (c) above with the substitution of $Cu(NO_3)_2$ for $CuCl_2$.

f. Tris(ethylenethiourea)copper(I)sulfate: This compound was prepared by the method described in (c) above with the substitution of $CuSO_4$ for $CuCl_2$.

g. Tris(thiourea)copper(I)chloride: A minimum amount of boiling water was used to dissolve 0.45 mole of thiourea. (EKC No. 5955). This solution was added to a solution of 0.1 mole $CuCl_2 \cdot 2H_2O$ prepared in an identical manner. The resulting reaction mixture was filtered hot to remove sulfur and cooled in an ice bath. The white crystals which formed were filtered by suction, and recrystallized from hot water.

h. Bis(thiourea)chloride, bromide and nitrate: All of these compounds were prepared by the procedure described in (g) with the amount of ligand being limited to 0.35 mole.

B. Instrumentation

1. Superregenerative Zeeman-Modulated Spectrometer

In order to provide a suitable means for searching for nuclear quadrupole resonance lines, a source of radiofrequency power which is both reasonably stable and sensitive over a wide frequency range is needed. For searching purposes a superregenerative oscillator-detector system is usually employed.

The underlying principle of the superregenerative spectrometer has been described by a number of authors[28,14]. The system used has been described by Croston[6]. The general operation will be briefly reviewed. The unique characteristic of a superregenerative oscillator is the periodic quenching of the oscillations. This results in there being a period of time during which the oscillations are cut off followed by a period when the oscillations build up from a low level to some maximum value. Such repetitive build-up of oscillations is accomplished by means of either large negative pulses being applied to the grid of an ordinary cw oscillator tube (external quenching) or the RC time constant in the grid circuit is made sufficiently large to allow the necessary negative voltage to develop on the grid before the capacitor is discharged (internal or self-quenching). When these periodically quenched oscillations are subjected to absorption by the sample, the maximum oscillation amplitude is decreased. At the same time, if the relaxation time for the nuclear signal in the sample is shorter than the quench period, oscillations build up from the noise rather than the decaying nuclear signal and incoherent operation results. On the other hand, if the relaxation time for the nuclear

signal is longer than the quenching period, the oscillations then build up from the tail of the dying nuclear signal and coherent operation results. The maximum amplitude of the oscillation is then effectively determined by the nuclear absorption.

In order to be able to detect the difference in oscillation amplitude between absorbing and nonabsorbing conditions, Zeeman modulation is provided. A periodic magnetic field created by a square wave of current is applied to a Helmholz magnet surrounding the sample coil of the oscillator system. The absorption of a powdered sample will be broaden and its intensity reduced to zero by the magnetic field if the magnetic field is on and the nuclear absorption will be present if the magnetic field is off. The effect of the modulation is to amplitude modulate the rf-signal. The oscillator output is then filtered to remove the rf- and quench frequencies and the remaining component, which is at the modulation frequency is amplified and recorded.

A block diagram of the spectrometer circuit is shown in Figure 13.

2. Method of frequency measurement:

Two methods have been used for frequency measurements and have given consistent results on both the samples studied and known compounds. (1) Frequency measurements were made by setting the oscillator on the center of a resonance line and converting the oscillator to cw operation by the imposition of a large dc voltage to the control grid. The oscillator frequency was then measured with a Hewlett Packard 5245L frequency counter. For known resonance this method gives

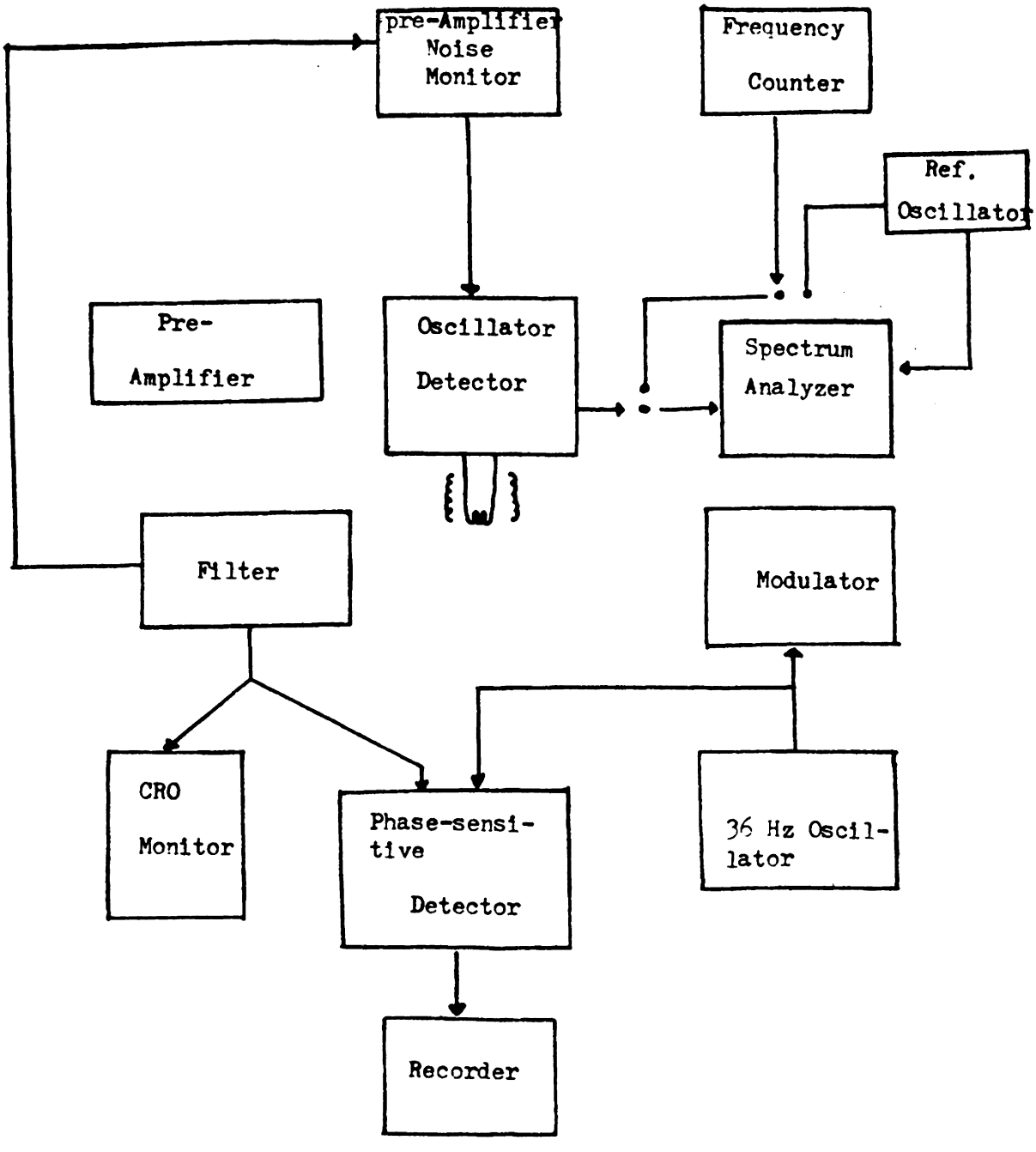

FIGURE 13

Block Diagram of Superregenerative NQR Spectrometer

agreement to ±0.002MHz. (2) The resonance frequencies were also measured by using a system involving an external reference oscillator and a spectrum analyzer. The multiple sideband spectrum of the super-regenerative oscillator which results from the quenching action, and is illustrated in Figure 14, is observed on the screen of a high resolution spectrum analyzer which is coupled to the oscillator. The center frequency, f_c, is the frequency to which the oscillator is tuned and is the frequency of interest in any measurement. The sidebands are separated from f_c by multiples of the quench frequency, f_q, and exhibit decreasing amplitude as the order of the sideband increases. A variable frequency oscillator (VFO) is also coupled to the high resolution spectrum analyzer and serves as a reference frequency source. When the reference frequency f_r is coincidental with the frequency f_c, as observed on the analyzer oscilloscope, the former frequency is measured with the frequency counter. The limitation on the frequency measurements is that of setting the spectrometer on the peak of an absortion line. This is of the order of 10% of the quench frequency or ±0.002MHz.

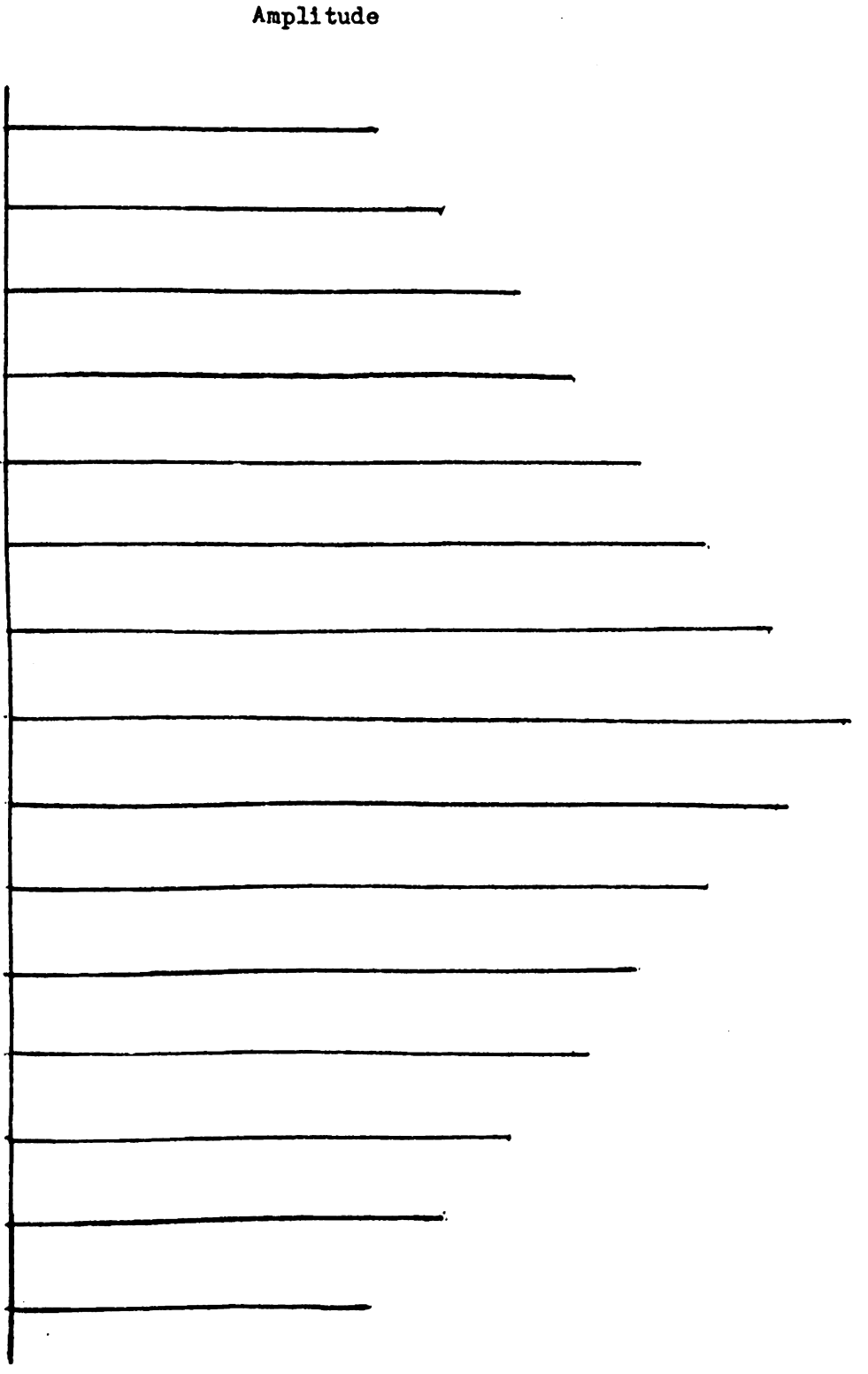

FIGURE 14

Spectrum of a Superregenerative Spectrometer

C. NQR Data

1. The bis(tetracarbonylcobalt)tin compound were searched for the nuclear quadrupole resonance frequencies over a range of 5-40 MHz at room temperature. Table XV gives the compounds investigated and the resonances found. Figures 15 through 17 show typical resonance patterns obtained. The cuprous oxide resonance at 26.020MHz was used to check the sensitivity and the resolution of the spectrometer. The lowest pair of resonances for the chlorophenyl and diphenyl compounds could not be found due to their low intensity. All of the compounds studied had very low intensities. In order to improve the observed intensities the sample coils were wraped tightly around the samples to maximize the coil filling factor. Also very low scanning speed and long time constants were used to obtain maximum response.

2. The copper(I) coordination compounds were searched for nuclear quadrupole resonance frequencies over a range of 10-60MHz at room temperature. The compounds studied along with the observed frequencies are given in Table XVI. The intensities of the observed frequencies varied. Both $Cu(etu)_2Cl$ and $Cu(etu)_{4\ 2}(So_4)$ were also searched at liquid nitrogen temperature by using a cold finger dewar. Figures 18 through 20 show typical resonance patterns obtained.

TABLE XIV

NQR Parameters for Bis(tetracarbonylcobalt)tin (IV) Compounds

Compound	^{59}Co Resonance Frequencies (MHz)[a] $_1$(S/N)	$_2$(S/N)	$_3$(S/N)	^{35}Cl Resonance Frequency (MHz) (S/N)
$Cl_2Sn[Co(CO)_4]_2$	10.853 (5)	21.243 (8)	31.926 (8)	17.676 (3)
	10.516 (5)	20.607 (8)	30.988 (8)	17.150 (3)
$Cl\phi Sn[Co(CO)_4]_2$	b	18.356 (2)	27.500 (2)	b
	b	18.100 (2)	27.250 (2)	
$\phi_2Sn[Co(CO)_4]_2$	b	16.075 (2)	24.219 (2)	
	b	16.030 (2)	24.089 (2)	

[a]Experimental error for all frequencies is ±0.004 MHz.

[b]Not observed.

FIGURE 15

NQR Spectrum of ^{35}Cl in $Cl_2Sn\ Co(CO)_{4\ 2}$, 25°C,

0.2MHz/hr Scan Speed, 3 sec. Time Constant

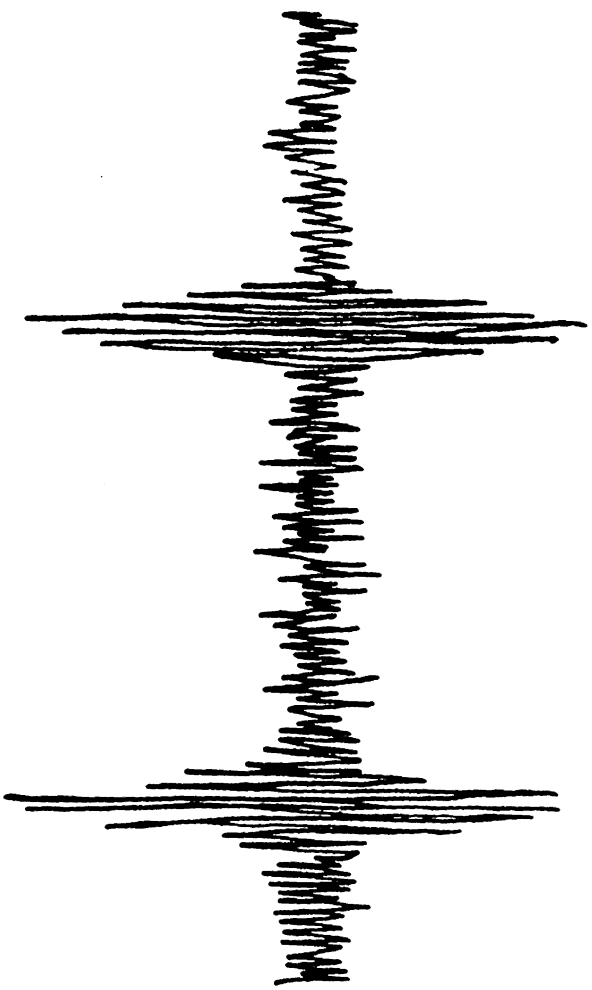

FIGURE 16

NQR Spectrum of $^{59}Co(5/2\text{-}7/2)$ in $Cl_2Sn\ Co(CO)_{4\ 2}$, 25°C, 0.2MHz/hr Scan Speed, 3 sec. Time Constant

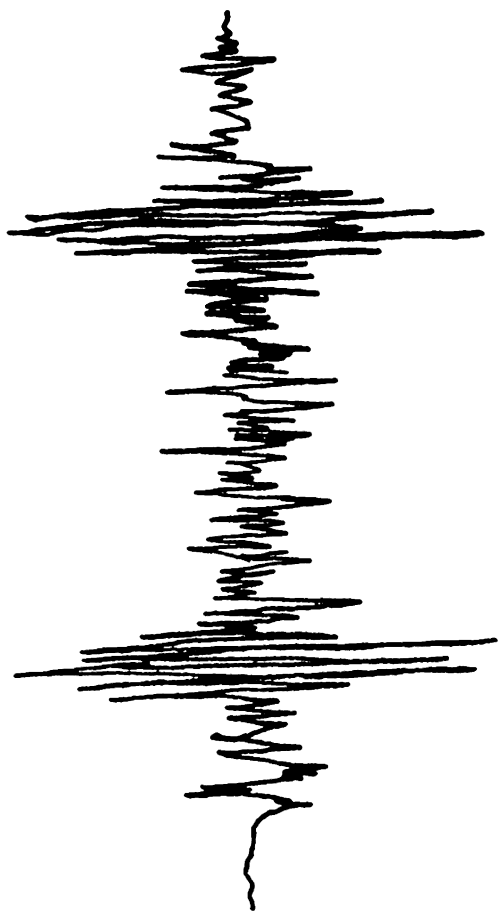

FIGURE 17

NQR Spectrum of ^{59}Co (1/2-3/2) in $Cl_2Sn\ Co(CO)_4$ 2 25°C,

0.2MHz/hr Scan Speed, 3 sec. Time Constant

TABLE XV

Observed NQR frequencies for Cu(I) Complexes

	^{63}Cu	^{65}Cu	S/N(^{63}Cu)
$Cu(tu)_2NO_3$[a]	25.088 MHz	23.280	5/1
$Cu(etu)_2Br$	32.010	29.620	20/1
$Cu(etu)_2Cl$	27.860	25.753	50/1
$Cu(etu)_4{}_2SO_4$	31.562	29.250	20/1
$Cu(tu)_2Cl$[b]	22.115 19.296	20.40 -	- -
$Cu(etu)_2ClO_4$	22.881	-	3/1
$Cu(tu)_2Br$	16.443 16.181	- -	3/1 3/1
$Cu(dmtu)_3Cl$	38.804	36.825	5/1

[a] tu = thiourea; etu = ethylenethiourea; dmtu = N,N'dimethylthiourea

[b] G.L. McKown & E. Swiger, Private Communication.

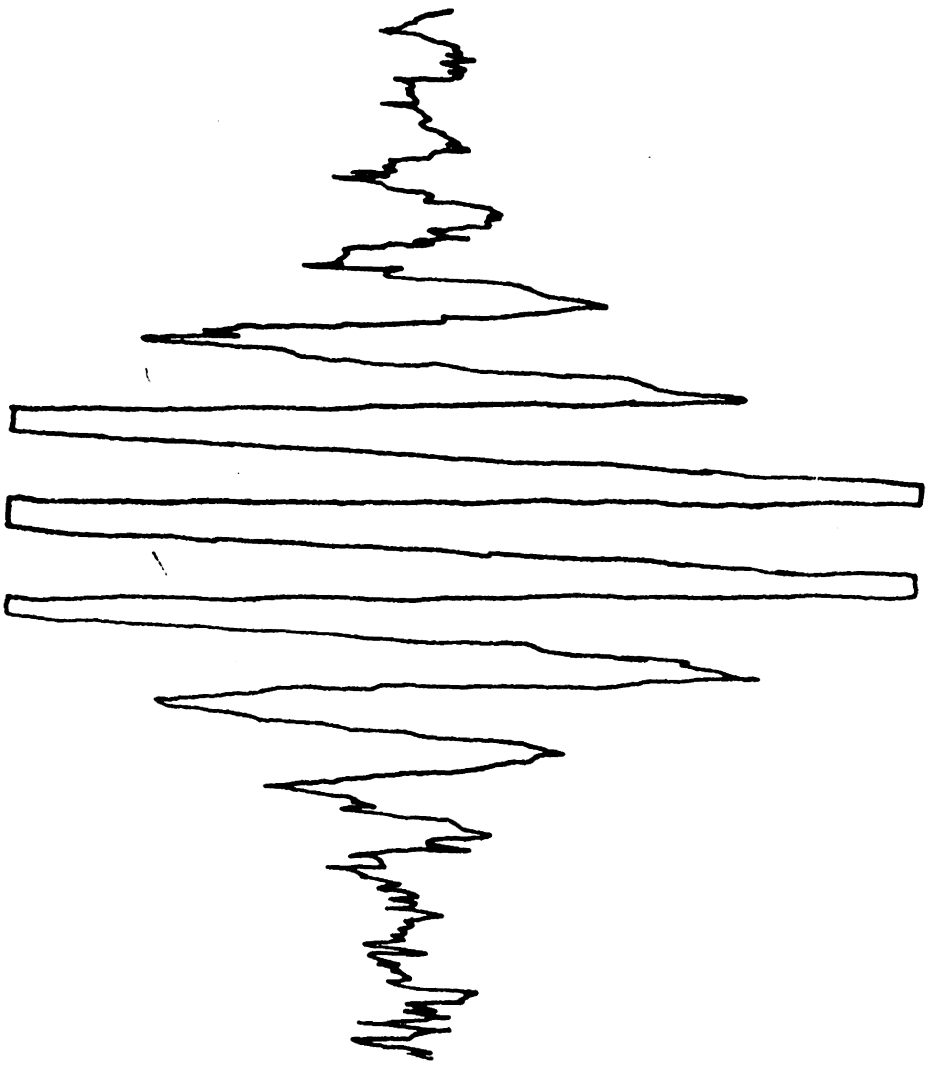

FIGURE 18

NQR Spectrum of ^{65}Cu in $Cu(etu)_2Cl$, 25°C,

0.05MHz/hr Scan Speed, 1 sec. Time Constant

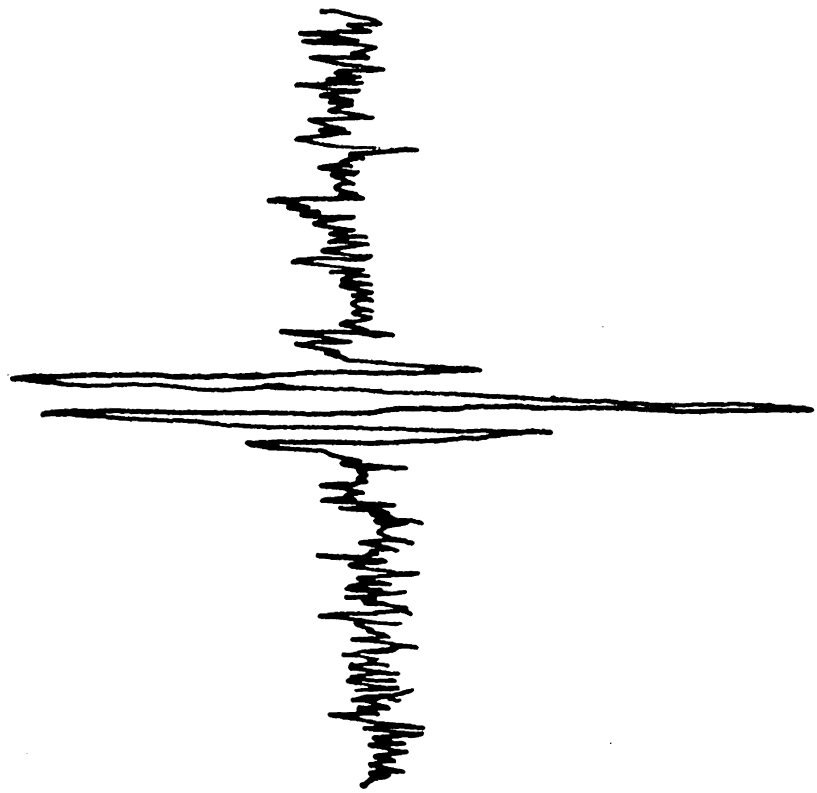

FIGURE 19

NQR Spectrum of ^{65}Cu in $Cu(etu)_4{}_2SO_4$, 25°C,

0.1MHz/hr Scan Speed, 1 sec. Time Constant

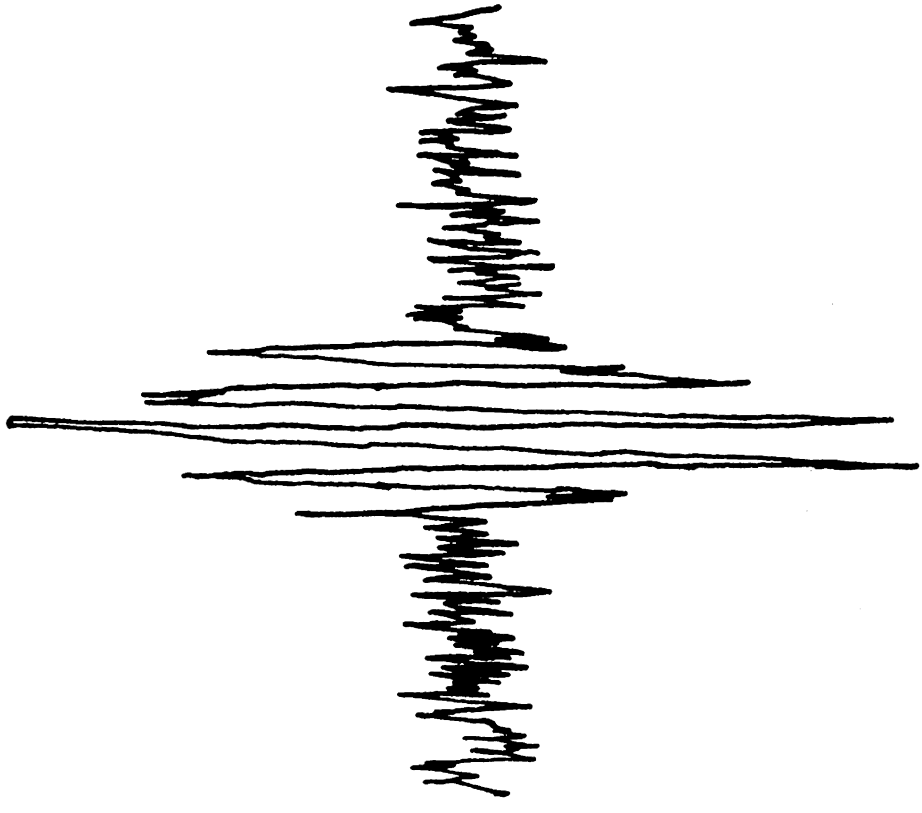

FIGURE 20

NQR Spectrum of ^{79}Br in $Cu(etu)_2Br$, 25°C,

0.1MHz/hr Scan Time, 1 sec. Time Constant

3. The range of 5-95MHz was searched using the molybdenum oxyhalides (Climax Molybdenum Co. - used as received). The compounds studied and the resonance frequencies found are tabulated in Table XVII. The intensities of the resonance frequencies are low due to the low natural abundances of both $I=5/2$ isotopic species of Mo. Figure 21 shows the broad Mo resonance in $MoOCl_4$.

TABLE XVI

Observed NQR Frequencies in Molybdenum Compounds

Compound	Mo		Cl
	$\frac{1}{2} - \frac{3}{2}$	$\frac{3}{2} - \frac{5}{2}$	
$MoOCl_4$	17.243 MHz	36.562 MHz	19.319 MHz
MoO_2Cl_2	16.127	35.877	

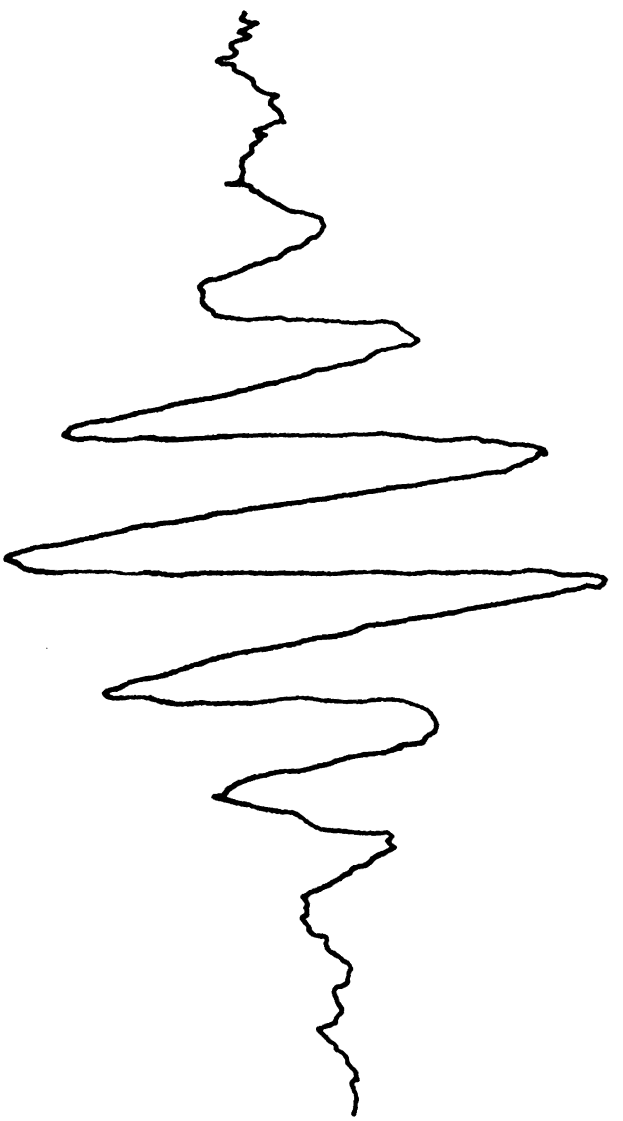

FIGURE 21

NQR Spectrum of a Mo Isotope in $MoOCl_4$

25°C, 0.05MHz/hr Scan Time, 1 sec. Time Constant

DISCUSSION

A. Bis(tetracarbonylcobalt)tin compounds

The observed resonances are given in Table XV for ^{59}Co, which has a nuclear spin I = 7/2. Both e^2Qq_{zz} and η were obtained from the experimental frequencies by use of the series approximations for the transition frequencies given in Table II. These values were further confirmed by using the frequency ratio plot of the type discussed earlier and shown in Figure 22. The frequency ratios for η = 0.1 to 0.5 are given in Table III. The asymmetry parameters for ^{59}Co and the frequency ratios as experimentally determined are given in Table XVIII.

The occurance of two closely spaced resonances for each compound indicated two nonequivalent crystallographic sites for the Co atoms in each. The crystal structure of $SiCl_3Co(CO)_4$ is known The Co atom occupies a site having trigonal (C_{3v}) point symmetry in this compound. If we assume that this trigonal environment is retained in the cobalt atom in the bistetracarbonyl compounds then the symmetry parameter, η, be equal to zero. The fact that the experimentally observed η values are not equal to zero but have some small values indicate that the 3-fold symmetry has been distorted slightly. Such a distortion might be due to non-trigonally symmetric intermolecular forces in the crystalline solids, intramolecular effects, or crystal packing eliminating the strict C_{3v} symmetry of the Co sites. If distortion of the intramolecular bonding caused deviations of the cobalt sites from C_{3v} symmetry then all inequivalent sites should have

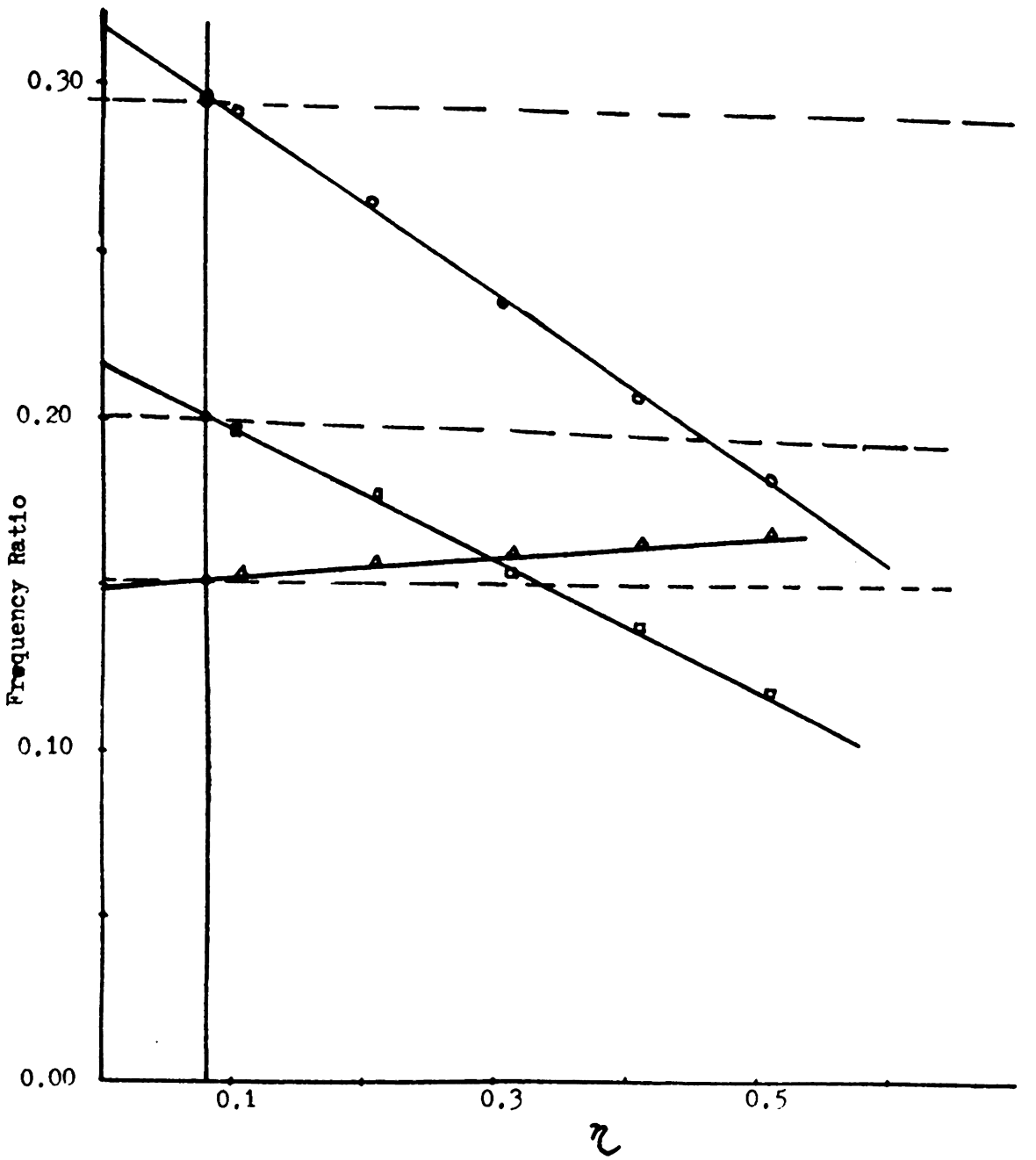

FIGURE 22

Frequency Ratio vs Asymmetry Parameter Plot for ^{59}Co in $Cl_2Sn\ Co(CO)_4$ 2

TABLE XVII

Experimental Observed Frequency Ratio and the Asymmetry Parameter Determined From Figure22

Compounds	$\frac{5/2-3/2}{3/2-1/2}$	$\frac{7/2-5/2}{5/2-3/2}$	$\frac{7/2-5/2}{3/2-1/2}$	η
$Cl_2Sn[Co(CO)_4]_2$	1.9565	1.5036	2.9420	0.065
	1.9491	1.5038	2.9382	0.074
$Cl\phi Sn[Co(CO)_4]_2$	--	1.5055	--	0.051
	--	1.4981	--	0.089
$\phi_2Sn[Co(CO)_4]_2$	--	1.5008	--	0.094
	--	1.5035	--	0.063

the same η values. The observed η values are different for inequivalent sites in the same compound and the differences are of the same order of magnitude as the value of η. This leads one to conclude that intermolecular forces rather than intramolecular effects causes the occurance of multiple resonances in each compound. In effect, the occurance of the low values of η leads to the conclusion that the cobalt site symmetry can be considered as C_{3v}.

There are two methods one can use to discuss the chemical bonding in these compounds:

1. Compare the experimental parameters with those of similar compounds. This method serves to point out chemical trends and substitution effects.

2. Consider the quadrupole coupling constants in terms of the occupancy of atomic orbitals. This method allows one to formulate the quadrupole coupling constants in terms of the contribution of electrons in the different types of bonding orbitals and to vary the electron densities in the bonding orbitals to get the best possible agreement between calculated and observed coupling constants.

Table XIX lists the e^2Qq_{zz} and η values for the compounds studied along with those of several related compounds. This data can be used for a comparison of the type just mentioned. The inductive effect of a Cl atom bonded to a Sn atom will increase the electron affinity of the empty 4d orbitals of the Sn atom. This will tend to drain electron density from the filled 3d-orbitals and in turn will remove electron density from the CO π*-orbitals. The net effect will be to (a) free some of the s-electron density of the tin atom from the

TABLE XVIII

NQR Data for Tin Compounds

Compound	$e^2Qq_{zz}(^{59}Co)$[a] (MHz)	$e^2Qq_{zz}(^{35}Cl)$[a] (MHz)	(Co)	(Cl)	Ref.
$Cl_2Sn[Co(CO)_4]_2$	146.9	30.0[f]	0.070		
$Cl\phi Sn[Co(CO)_4]_2$	127.7	-	0.070		
$\phi_2Sn[Co(CO)_4]_2$	112.9		0.078		
$Cl_3SnCo(CO)_4$	163.45	39.76[f]	0.0		b
$\phi_3SnCo(CO)_4$	104.11		0.05		b
$ClSn[Co(CO)_4]_3$	1.35.9		0.09		g
$SnCl_4$		47.7		0.25	c
$Cl_2Sn(CH_3)_2$		30.8		0.34	d
$Cl_2Sn\phi_2$		35.7[f]		-	e

a. Average for multiple resonances.
b. T.L. Brown, P.A. Edwards, C.B. Harris and J.L. Kirsch, Inorg. Chem., 8, 763 (1969).
c. J.D. Graybeal and P.J. Green, J. Phys. Chem., 73, 0000 (1969).
d. J.D. Graybeal and B.A. Berta, Proceedings 2nd Materials Research Symposium, National Bureau of Standards, 1967, p. 383.
e. P.J. Green and J.D. Graybeal, J. Am. Chem. Soc., 89, 4305 (1967).
f. Assumed $\eta = 0$.
g. D.D. Spencer, J.J. Kirsch and T.L. Brown, J. Inorg. Chem., 9, 237 (1970).

Sn-Cl bond and make it more available in the Sn-Co bond, (b) decrease the net electron population of the Co atom, and (c) strengthen the C≡O bond. These effects will result in (a) an increase of the Co-Sn-Co-bond angle, (b) an increase in $e^2Qq_{zz}(Co)$, and (c) an increase in the C-O stretching frequency with increased Cl substitution. The first and third points have been substantiated by Patmore and Graham[35] while this work confirms the second.

2. The replacement of a $Co(CO)_4$ group by a Cl atom show a substantial increase in the coupling constant of cobalt atom further confirming the concept of reduced electron density on the Co atoms due to halogen inductive effect.

3. The value of $e^2Qq_{zz}(Cl)$ increases going from $Cl_2Sn(Co(CO)_4)_2$ to $SnCl_4$ rather than decreases as one might expect if the Cl atom gained electron density. This observed change indicates that the net electron density change on the Sn atoms is relatively small and is insufficient to provide any net increase of electron density on the Cl atoms in view of increased competition of the large number of Cl atoms.

4. Substitution of a phenyl group for the $Co(CO)_4$, results in a increase of $e^2Qq_{zz}(Co)$ at the remaining cobalt atom. Brown[47] has pointed out that the substitution of a methyl group for a phenyl group has the same effect on the remaining Co-atom. On the basis of the $e^2Qq_{zz}(Co)$ values, the $Co(CO)_4$ group is a better electron withdrawing group than either the phenyl or the methyl groups. The following series, in order of decreasing electron withdrawing ability, can be established for compounds of the type studied.

$$Cl \approx Br > Co(CO)_4 > \phi > CH_3$$

The magnitude of the observed coupling constant can be rationalized on the basis of a simplified calculation of the EFG tensor components and the use of an electronically analogous system to estimate orbital electron populations. The molecular field gradient, q_{zz}, can be expressed in terms of the various type of 3d and 4p electrons by using the relationship of the field gradient to angular momentum. In either a

$$q_{nlm} = q_{nl0}\left[(1-3m^2)/l(l+1)\right] \qquad (56)$$

valence bond or molecular orbital approach, q_{zz} arising from the 3d and 4p electrons can be expressed in terms of atomic orbital populations, N_j

$$q_{zz} = q_{320}\left[N_{d_{z^2}} + 1/2\,(N_{d_{z_x}} + N_{d_{z_y}}) - N_{d_{x_y}} + N_{d_{x^2-y^2}})\right] + q_{410}\left[-\frac{(N_{p_x} + N_{p_y})}{2} + N_{p_2}\right] \qquad (57)$$

The coupling constant is given by

$$e^2Qq_{zz} = eQq_{320}\left[N_{dz^2} + 1/2(N_{d_{x_z}} + N_{d_{y_z}}) - (N_{d_{x_y}} + N_{d_{x^2-y^2}})\right] + e^2Qq_{410}\left[-\frac{(N_{p_x} + N_{p_y})}{2} + N_{p_2}\right] \qquad (58)$$

A.F. Schreiner[46] has calculated the electron densities for $Fe(CO)_5$. These are given in Table XX. This is an isolectronic and isostructural compound to the bis(tetracarbonylcobalt)tin compounds. By using the electron densities calculated by Schreiner, hydrogen-like wave functions and an effective atomic number of Co given by Korol'kov and Makhanek[23],

TABLE XIX

Orbital Populations in $Fe(CO)_5$

Orbital	Population	Orbital	Population
$3d_{z^2}$	1.23	$4p_z$	0.07
$3d_{xz}$, $3d_{yz}$		$4p_x$, $4p_y$	0.17
$3d_{xz}$, $3d_{x^2-y^2}$		4s	0.27

the atomic coupling constant, e^2Qq_{320}, is estimated to be 192 MHz. The magnitude of q_{410} is less than one-fifth that of q_{320}[46]. The atomic coupling constant e^2Qq_{410}, is estimated to be 12 MHz. The total coupling constant as found by using Equation 58 is 204MHz.

This calculated value is related to the observed value by

$$(e^2Qq_{zz})_{obs.} = (1-R)\ (e^2Qq_{zz})_{calc.}$$

where R is the Steinheimer shielding factor for an open-shell system. Calculations to date show $-0.3 < R < 0.2$. When one considers that the lower electronegativity of tin, as compared to carbon, would probably result in $N_{d_{z^2}}$ being larger in these compounds as compared to the completely symmetric type, the estimate of e^2Qq_{zz} is reasonable.

B. Copper(I) thiourea and substituted thiourea complexes

Table XVI lists the observed frequencies of the compounds studied. A number of interesting observations regarding these observed frequencies can be made. 1) There is appreciable variation among the observed frequencies of those compounds which might be considered as belonging to an isomorphous series. 2) The frequencies are in the vicinity of the reported values for Cu_2O (26.02 MHz) and $KCu(CN)_2$ (33.468 MHz). 3) There are two absorption frequencies for the bis-compounds of thiourea with copper halides and one frequency for the other compounds. 4) The observed absorption frequencies for substituted thiourea complexes, in general, are higher than the thiourea complexes. 5) There is a reversal of the order of the frequencies between the pair, bis(thiourea)Copper(I) chloride and bromide and the pair, bis(ethylene-thiourea)Copper(I)chloride and bromide.

2) Since all of the atomic orbitals to be considered fall into groups having the same principal quantum numbers the radial parts are common, and the angular and the radial parts are seperable, the radial part is given by an expression originally developed by Pauling[20].

$$e\left\langle \frac{1}{r^3} \right\rangle = \frac{2 Z_e^3 e}{n^3 a_o^3 l(l+1)(2l+1)} \qquad (60)$$

where n = principal quantum number

l = azimuthal quantum number

A_o = the Bohr radius

Z_e = effective atomic charge = Z-s, s is the screening constant, and the angular part,

$$q_{ns} = \frac{3}{4} \int_o^{\pi} \int_o^{2\pi} \psi^*_{lm} [q_{rs}]_{op} \psi_{lm} \sin\theta d\theta d\phi \qquad (61)$$

3) The radial contribution is evaluated for Cu(I), which has an electronic configuration $4s^0 3d^{10}$, by using the slater rules given by Kauzmann[20] in order to evaluate the necessary screening constant. The screening constant is calculated to be 25.3, with the effective atomic charge being

$$Ze = 29 - 25.3 = 3.7.$$

The radial contribution is then

$$e\left\langle \frac{1}{r^3} \right\rangle = \frac{2X(3.7)^3 \text{ X } 4.8 \text{ X } 10^{-10}}{4^3 \text{ x } (5.3 \text{ X } 10^{-9})^3 \text{ X } (1+1)(2+1)} = 8.56 \times 10^{14} \text{ esu cm}^{-3}.$$

4) The angular part of the atomic were functions are given in Table XXII. The angular contribution to q_{rs} can be calculated as shown by the following example:

Having enumerated the pertinent features regarding this work possible explanations will now be considered. 1) The variations that are observed among compounds such as $Cu(etu)_2Cl$, $Cu(etu)_2Br$ and $Cu(etu)_2NO_3$ are of sufficient magnitude to indicate that there is an appreciable anion effect operable. This is concluded since the magnitudes of the differences are greater than normal differences due to non-equivalent crystallographic sites.

2) The occurance of the observed resonance frequencies in the vicinity of those of Cu_2O and $KCu(CN)_2$, lead one to conclude that the bonding is probably similiar. Prior work on these compounds by other investigators indicate predominantely covalent bonding in Cu_2O and predominantely covalent bonding in the $Cu(CN)_2^-$ ion of $KCu(CN)_2$. This evidence for covalent bonding forms the basis of later discussions of the bonding.

3) The reason for the occurance of two frequencies for the bis-compounds is different from that which gave rise to the two closely spaced frequencies which were discussed in the cobalt compounds. For the copper compounds their appearance is due to the occurance of two distinctly inequivalent chemical sites and not to intermolecular interactions or crystal packing effects. This point is substantiated by crystal structure studies on the bis(thiourea)Copper(I) chloride. The $Cu(tu)_2^+$ species form infinite spiral chains with the Cu-Cu separations alternating between a long and a short internuclear distance with accompanying "broad" and "sharp" Cu-S-Cu angles. This alternation of bond distances along with that of the angles is a strong indication that the copper atoms are situation in two different chemical sites. On the

basis of the crystal study of the bis(thiourea)chloride and the observation of two frequencies for each bis-compounds one is lead to conclude that all of the bis-compounds have structures similar to bis(thiourea)Copper(I) chloride, i.e. they form infinite spiral chains with the copper atoms situated in tetrahedral sites with alternate broad and sharp angles. If one accepts this conclusion, one would expect two frequencies for the bis(thiourea)Copper(I) nitrate also. The experimental result however shows only one frequency and therefore indicates one chemical site for the copper atom. The reason for this is not known. A possible explanation could be that the size of NO_3^- ion is such that the compound cannot form the same type structure as the halides and may possibly form a discret structure similar to the tris(N,N'dimethylthiourea)copper(I) chloride.

4) The higher NQR resonance frequencies for the substituted compounds can be rationalized in terms of the inductive effect of the substituents on the thiourea ligand. Figure 22 shows the resonance forms of thiourea, ethylene thiourea and N,N'-dimethylthiourea. It was pointed out by Dr. Philip Hall in a private discussion, that the order of stability of the resonance form having charge separation are I II III. On the basis of the resonance forms, one would expect that I will contribute more electrons to the copper atom to form a complex than either II or III. Consequently, the copper atom will have the least p-electron defect if it forms complexes with I. Since the higher the p-defect, the higher the frequency, the observed frequencies are then in good agreement with this concept.

5) The reversal of the frequencies of the halogen complexes is difficult to explain on the basis of the electronegativity of chlorine

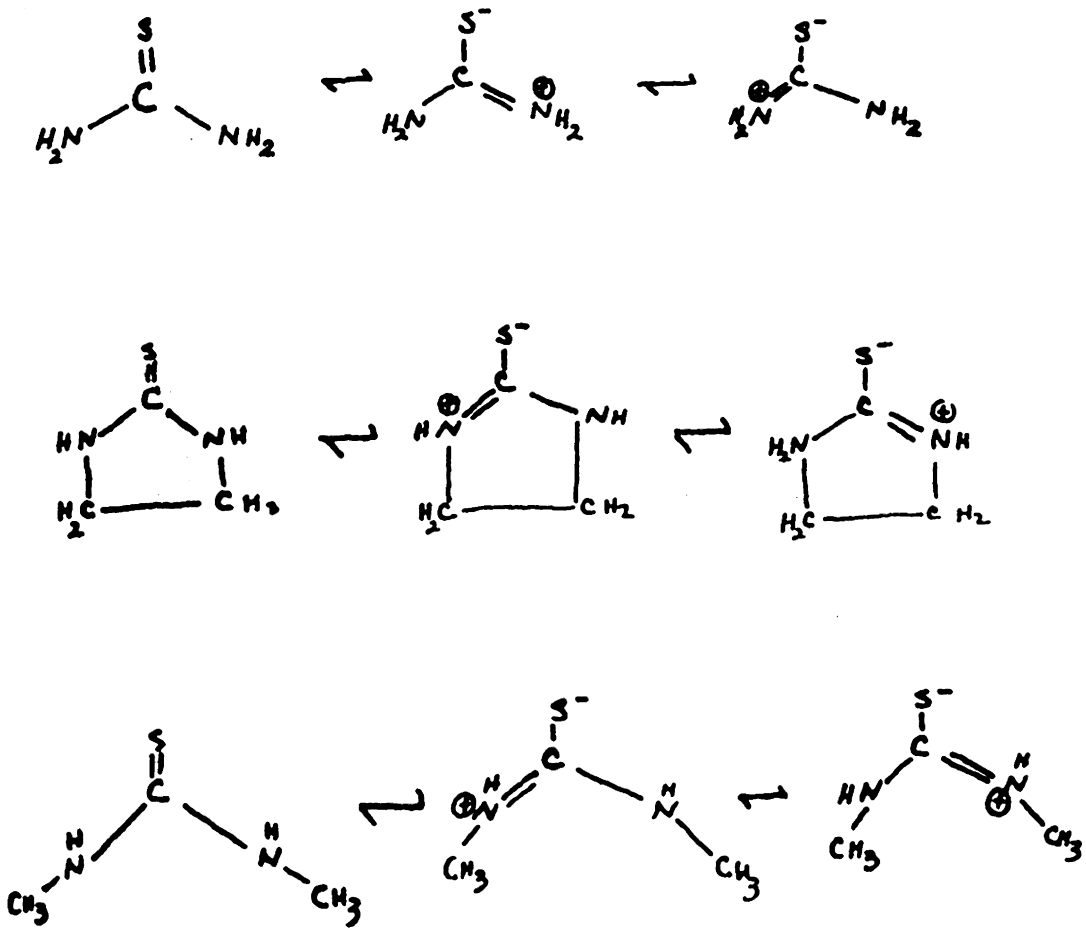

FIGURE 23

Resonance Forms of Various Ligands

or bromine. Since chlorine is more electronegative than bromine, one would expect the chlorine atom to withdraw electrons away from the copper atom more than the bromide ion if the Cu-X bond were subtaintally covalent. Consequently, the coupling constant or the resonance frequency should be lower for the chlorine compound in both cases. For those compounds whose structures have been determined the Cu-Cl bond length is such that appreciable ionic character is indicated. An approximate calculation, based on the assumption that all four compounds have the same structural configuration as the bis(thiourea)copper(I)chloride, i.e. the copper atom is situated at a tetrahedral site, with three covalently bonded ligands at three corners of the tetrahedron and the chloride or bromide ion at the fourth corner, shows that the contribution to the EFG tensor component, q_{zz}, varies with the internuclear distance between Cu and Cl as shown in Figure 23. At a particular internuclear distance, q_{zz} goes through a minimum. This calculated minimum indicates that q_{zz} can increase with either a decrease or an increase of the internuclear distance of Cu-X. It is therefore believed that the electronegativity of the chlorine or bromine has relative little or no effect on the reversal of the order of the coupling constants. The reversal is probably due to the particular values of the Cu-X distances in the compounds. In view of the lack of the crystal structure data, the above explanation at it best, a speculation.

Finally, the observed ^{79}Br and ^{81}Br resonance at 38.828 and 46.588 MHz respectively, for bis(ethylenethiourea)copper(I) bromide are worth of mentioned. A simple Townes Dailey calculation using Br_2 as a base, shows that the Cu-Br bond with 78% ionic character is in line with the suggestions of Amma and Knobler.

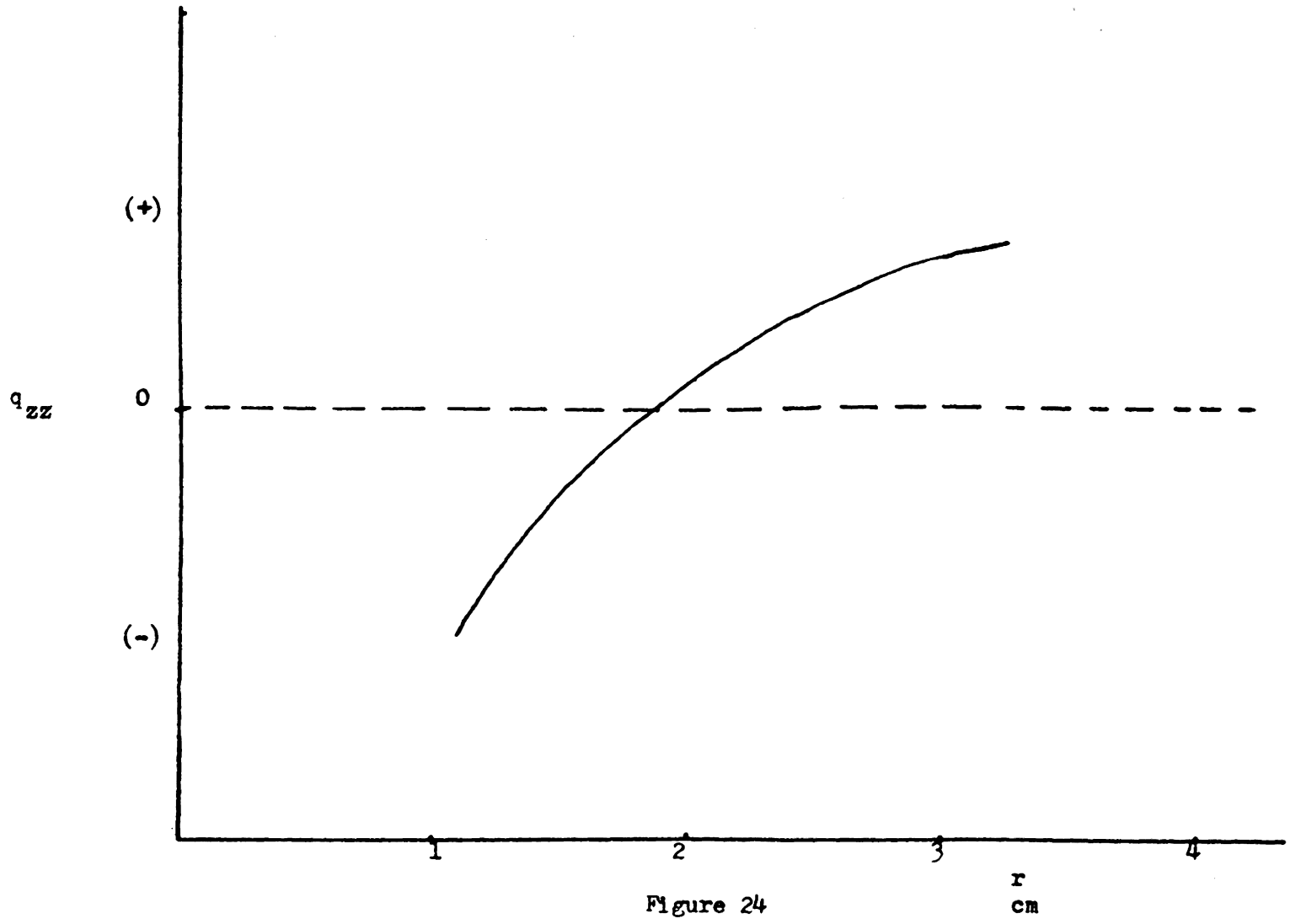

Figure 24

q_{zz}-EFG vs Internuclear Distance

The pure quadrupole resonance frequencies of ^{63}Cu and ^{65}Cu in bis(thiourea)copper(I)chloride were first reported by Swiger[51]. The crystal structure revealed a polymeric chain of alternating copper atoms and thiourea molecules with chloride interpersed. Amma[48] proposed a distorted sp^2-hybrid bond scheme for the Cu-S bonds and an ionic Cl. If this scheme is adopted for the bis(tu)Copper(I)chloride, the bond directions with respect to an arbitrary x, y, z axis system, (Figure 24) with the Cu-atom at the origin are given in Table XXI.

Following the method described on page 28 , and assuming a planar configuration, the choice hybrid orbitals for Cu-S bonds can be expressed in the following forms,

$$\psi_1 = 0.4935_s + 0.8651\ p_x$$
$$\psi_2 = 0.6155_s - 0.4255\ p_x - 0.7081\ p_y$$
$$\psi_3 = 0.6215_s - 0.4101\ p_x + 0.7055\ p_y.$$

These hybrid orbitals are both normalized and orthogonal. In order to determine the values for this contribution of a single electron to the principle z-EFG tensor component the EFG contribution due to one electron in each atomic orbital must first be evaluated. This is done as follows:

1) The contribution due to one electron in an atomic orbital described by a wave function, ψ_n, is found by the conventional quantum mechanical average method,

$$q_{rs}(\psi_n) = \int_0^{\infty}\int_0^{\pi}\int_0^{2\pi} \psi^*_{nlm}\,[q_{rs}]_{op}\,\psi_{nlm}\,\hat{n}^2 \sin\theta\, dr d\theta d\phi \qquad (59)$$

where $[q_{rs}]_{op}$ is the EFG operation (Table VI.)

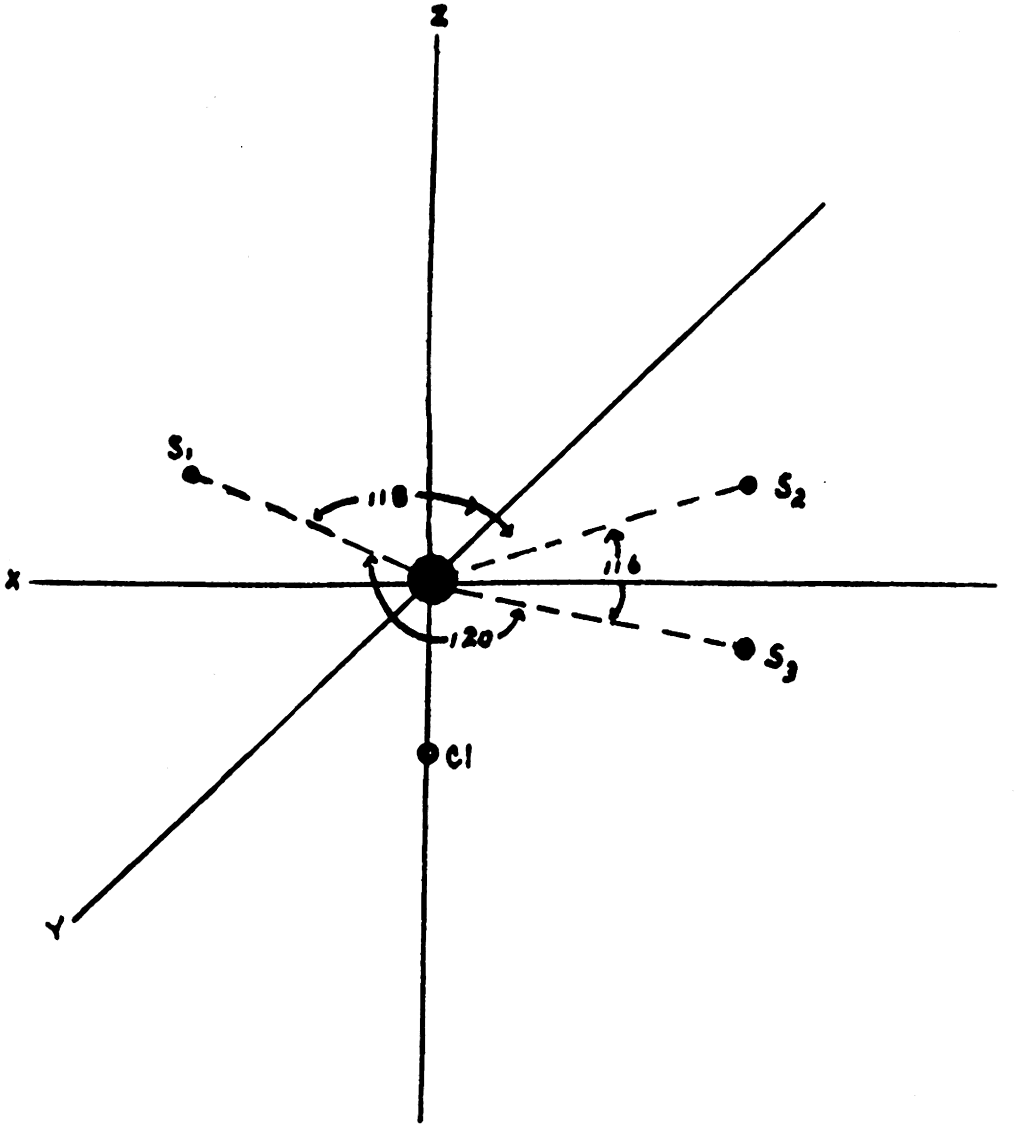

FIGURE 25

Orientation of Bonds in $Cu(tu)_2Cl$

TABLE XX

Bond direction of Cu-S and Cu-Cl bonds
with respect to x, y, z axis system

	x	y	z
$Cu-S_1$	90°	17°	107°
$Cu-S_2$	$29^\circ 29'$	120°	95°
$Cu-S_3$	$30^\circ 19'$	$119^\circ 19'$	87°
Cu-Cl	90°	90°	0°

TABLE XXI

Angular part of the atomic wave functions

$p_z = (\sqrt{3}/2\sqrt{\pi}) \cos\theta$	$p_y = \sqrt{3}/4\pi \sin\theta \cos\phi$
$p_x = \sqrt{3}/4\pi \sin\theta \sin$	$d_{z^2} = \sqrt{5}/16\pi (3\cos^2\theta - 1)$
$d_{x_z} = \sqrt{15}/16\pi (\sin 2\theta \cos\phi)$	$d_{y_z} = \sqrt{15}/16\pi (\sin 2\theta \sin\phi)$
$d_{y^2-y^2} = \sqrt{15}/16\pi \sin^2\theta \cos 2\phi$	$d_{x_y} = \sqrt{15}/16\pi (\sin^2\theta \sin 2\phi)$

$$q_{xx}^{p_x} = \frac{3}{4\pi}\int_0^{\pi}\int_0^{2\pi}\left[3\sin^2\theta\cos^2\theta - 1\right]\sin^2\theta\sin^2\phi\,\sin\theta\,d\theta d\phi \qquad (62)$$

Table XXIII summarizes the angular contributions.

5) The total contribution of one electron in a single atomic orbital is the product of the two individual contributions. The values are tabulated in Table XXIV.

6) The values for the contributions of single electrons in each hybrid orbital to the principal Z-EFG tensor component are calculated and given in Table XXV.

7) It is estimated from the electronegativity difference between the Cu and the S-atoms that the ionicity of the Cu-S bond is 13.5%. Consequently, the S-atom would contribute 0.87 electron to the Cu-atom if each of the three hybrid orbitals has an equal electron density. In view of the recent detailed crystal structure analysis done by Amma[48], the change density on the Cu- and the S-atoms are estimated and tabulated in Table XXVI. It was pointed out that one of the sulfur-atoms forms a three-center, two -electron-bridge bond with two Cu-atoms while the other two sulfur atoms each forms a Cu-S covalent bond with a Cu-atom. If one assumes equal electron density for these two Cu-S hybrid orbitals, the charge density on these two hybrid orbitals should be $\psi_1 = 0.87$ and $\psi_2 = 0.87$ electrons respectively. For the three-center, two electron bridge hybrid, the S-atom must supply both electrons to form the bridge bond. If this is indeed the case, the charge density of ψ_3 should be 0.43 electrons.

TABLE XXII

Angular contribution of one electron in a single atomic orbital

Atomic orbital	q_{xx}	q_{yy}	q_{zz}	q_{xy}	q_{xz}	q_{yz}
p_x	-0.8	+0.4	+0.4	0	0	0
p_y	+0.4	-0.8	+0.4	0	0	0
p_z	+0.4	+0.4	-0.8	0	0	0

TABLE XXIII

The total contribution of one electron in a single atomic orbital

Atomic orbital	q_{xx}	q_{yy} (esu cm^{-3} X 10^{-14})	q_{zz}
$4p_x$	-6.84	3.42	3.42
$4p_y$	+3.42	-6.84	3.42
$4p_z$	+3.42	3.42	-6.84

TABLE XXIV

The Contribution of a single electron in a Hybrid Orbital to the Z-EFG Tensor Component

Orbital	q_{zz}
ψ_1	2.22×10^{14} esu cm^{-3}
ψ_2	2.33×10^{14} esu cm^{-3}
ψ_3	2.27×10^{14} esu cm^{-3}

TABLE XXV

Estimated Orbital Populations and Charge Density

	No $d\pi - d\pi$ Bonding	$D\pi - d\pi$ Bonding assumed
ψ_1	0.87	0.87
ψ_2	0.87	0.87
ψ_3	0.43	0.43
π_1	-	0.5
π_2	-	0.5
$\delta^+(S_1)$	0.87	0.37
$\delta^+(S_2)$	1.74	1.74
$\delta^+(S_3)$	0.86	0.36
$\delta^-(Cl)$	-1.00	-1.00
$\delta^-(Cu)$	-1.17	-0.67

The $(q_{zz})^{cov}$ for the Cu-atom is then calculated to be 4.94×10^{14} esu cm^{-3} and 4.08×10^{14} esu cm^{-3} for no $d\pi - d\pi$ bonding and with $d\pi - d\pi$ bonding respectively. Taking into consideration the shielding effect for an open shell system, the observed $(q_{zz})_{Cu}$ is therefore expressed as

$$(q_{zz})^{Cov}_{ob} = (q_{zz})^{Cov}_{cal} (1 - R_{\infty})$$

$$= 4.94 \times (1 + 0.2)$$

$$= 3.95 \times 10^{14} \text{ esu } cm^{-3}$$

The Sternheimer shielding constant for an open shell system, R_{∞}, for Cu^{+} is not known. The value $R_{\infty} = -0.2$ is estimated from the calculated value of the group IA elements. Since Cu^{+} is isoelectron with K^{+} and $(R_{\infty})_{K^{+}} = -0.188$, it is therefore reasonable to assume $R_{\infty})_{Cu^{+}} = -0.2$.

8) We have so far neglected ionic contributions from the chloride, sulfur and Cu-atoms. By using the classical electrostatic espression

$$(q_{zz})^{ionic} = \frac{e(3\cos^2\theta - 1)}{r^3} \qquad (64)$$

where r is the internuclear distance of Cu-X and θ is the angle between the Cu-X bond and the Z-axis (X = Cl, S, Cu). The ionic Z-EFG tensor components were calculated and are tabulated in Table XXVII. The observed EFG Z-component due to ions is related to the calculated value by the Sternheimer shielding constant for a closed shell system, γ_{∞}, by

$$(q_{zz})^{ionic}_{obs} = (q_{zz})^{ionic}_{cal} (1 - \gamma_{\infty}) \qquad (65)$$

TABLE XXVI

Ionic Contribution of Cl, Cu and S to the q_{zz}-EFG Tensor Component

	with d - d assumption	without d - d assumption
Cu_I	-0.154×10^{14}	-0.27×10^{14} esu/cm^3
Cu_{II}	-0.06×10^{14}	-0.06×10^{14}
$\delta^+(S_1)$	-0.15×10^{14}	-0.34×10^{14}
$\delta^+(S_2)$	-0.68×10^{14}	-0.68×10^{14}
$\delta^+(S_3)$	-0.15×10^{14}	-0.34×10^{14}
$\delta^-(Cl)$	-0.42×10^{14}	-0.42×10^{14}
Total	-1.61×10^{14}	-1.99×10^{14}

The best calculated γ_∞ value for Cu^+ is -17.0[57]. The calculated nuclear quadrupole coupling constant due to both ionic and covalent contributions is given by

$$(e^2Qq_{zz})_{obs} = (e^2Qq_{zz})^{ionic}(1-\gamma_\infty) + (e^2Qq_{zz})^{cov}(1-R_{oo})$$

$$= \frac{4.8\times10^{-10}\times0.16\times10^{-24}}{6.627\times10^{-27}}((1.2)3.95\times10^{14} - (18)1.99\times10^{14}$$

$$= -36.0 \text{ MHz}$$

for no $d\pi - d\pi$ bonding and -30.53 MHz for the assumed $d\pi - d\pi$ bonding case. It was also observed that there were two resonance frequencies for the Cu-atom. Following the same procedure, the nuclear quadrupole coupling constants for the Cu-atom having $r_{CuCl} = 3.16$ were calculated to be +33.6 MHz and +28.03 MHz without $d\pi - d\pi$ bonding and with $d\pi - d\pi$ bonding respectively. The experimentally observed values for the Cu coupling constants are 44.28 and 40.22 MHz. In view of the uncertainties of both the $d\pi - d\pi$ bonding contribution and the Sternheimer effect, the calculated values are in good agreement with the observed values. One must finally point out that the difference between the calculated and observed values for two different sites are in excellent agreement, and indicate that the model used is a reasonable one.

The resonance frequency for both Cu^{63} and ^{65}Cu in tris(N',N-dimethylthiourea)copper(I)chloride were observed at 38.804 and 36.825 MHz. The crystal structure has been determined by Amma[48,49], Figure 25. It revealed a discreet tetrahedral structure with the Cu atom at the tetrahedral site. The bond lengths of the Cu-S bonds are the same and they form angles of 112° with the Cu-Cl bond. The bond directions in

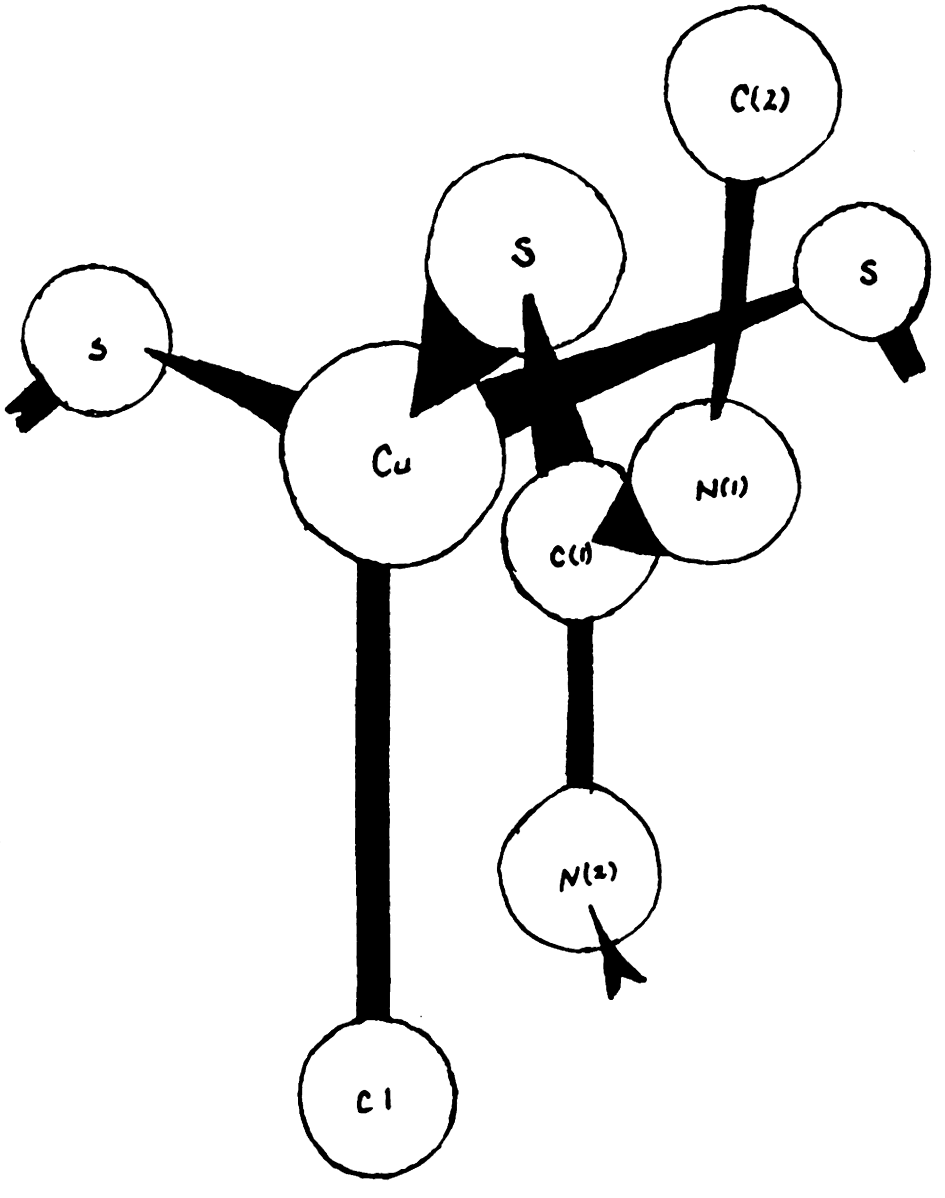

Figure 26

Structure of Bonds in $Cu(dmtu)_3Cl$

an arbitrary x, y, z axis are given in Table XXVIII, and shown in Figure 26.

An sp^3 hybrid scheme is adopted in evaluating the EFG tensor components at the Cu-atom in this system. The four hybrid orbitals are obtained by employing the same method as was used for the bis(thiourea)-Copper(I)chloride and are given by

$$\psi_1 = 0.5\,s + 0.866\,p_z$$
$$\psi_2 = 0.5\,s + 0.66\,p_x - 0.317\,p_z$$
$$\psi_3 = 0.5\,s - 0.245\,p_x + 0.707\,p_y - 0.317\,p_z$$
$$\psi_4 = 0.5\,s - 0.245\,p_x - 0.707\,p_y - 0.317\,p_z$$

The values for the contribution of a single electron to the principal Z-EFG tensor component in each of the hybrid orbitals were calculated as before and are given in Table XXIX.

From the electronegativity differences, The ionicity of the Cu-S bond is estimated to be 13.5% and that of the Cu-Cl bond is estimated to be 30%. Assuming an equal distribution of electron density in each of the Cu-hybrid orbitals bonded to sulfur atoms, the charge densities of the Cu and S-orbitals are estimated and given in Table XXX.

The $(q_{zz})^{cov}_{cu}$ for the Cu-atom is then calculated to be $(-0.94) \times 10^{14}$ esu cm^{-3}. Using the same Sterheimer shielding constant for the Cu-open shell system, the observed $(q_{zz})^{cov}_{cu}$ is expressed,

$$(q_{zz})^{Cov}_{obs} = (q_{zz})^{Cov}_{cal}\ (1 - R_\infty)$$
$$= 1.2 \times (-0.94) \times 10^{14} \text{ esu } cm^{-3}$$
$$= -1.13 \times 10^{14} \text{ esu}/cm^3$$

TABLE XXVII

Bond Direction of Cu-S and Cu-Cl Bonds With Respect to x, y, z Axis System

	x	y	z
$Cu-S_1$	98.54	109.57	112°
$Cu-S_2$	$98°.54^1$	$109°.57^1$	112°
$Cu-S_3$	$98°.54^1$	$109°.57^1$	112°
Cu-Cl	90°	90°	0°

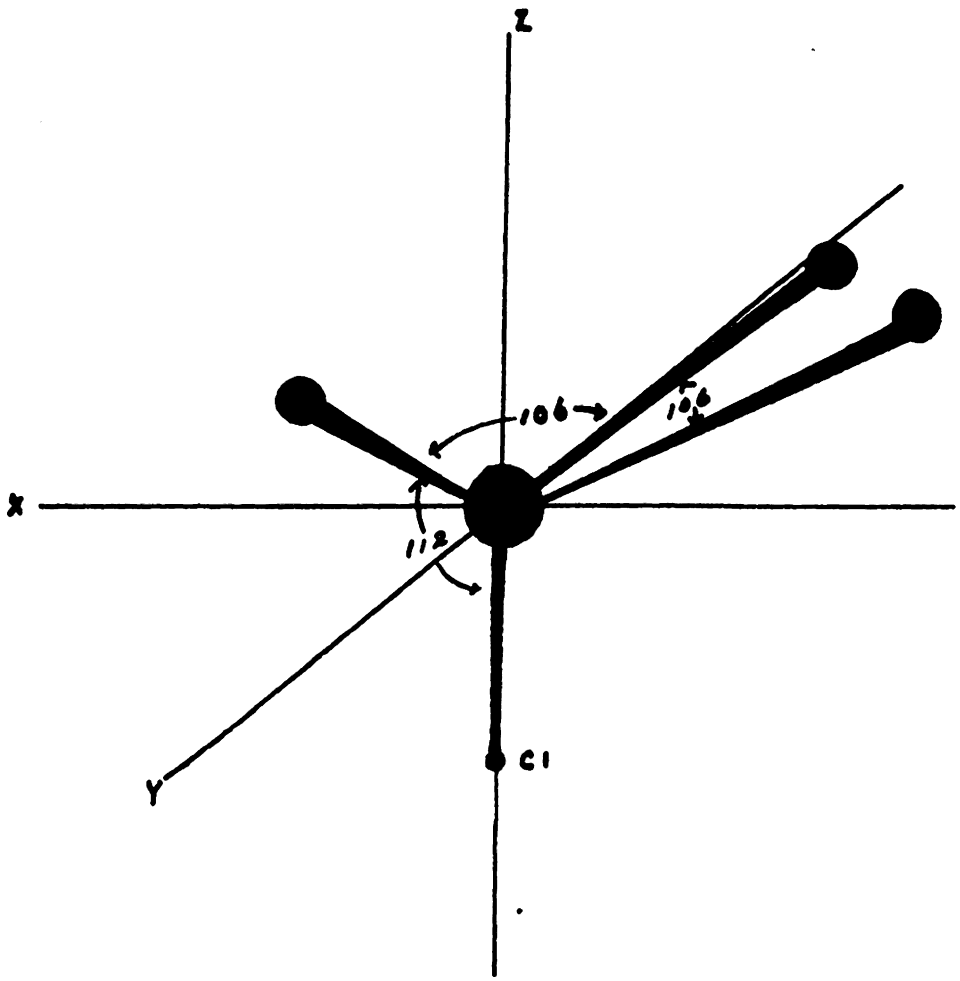

FIGURE 27

Orientation of $Cu(dmtu)_3Cl$

TABLE XXVIII

The Contribution of a Single Electron in a Hybrid -orbital to the Z-EFG Tensor Component

Bond (orbital)	$q_{zz})_{Cu}$
Cu-S_1 (ψ_2)	0.7×10^{14} esu/cm^3
Cu-S_2 (ψ_3)	1.24×10^{14}
Cu-S_3 (ψ_4)	1.24×10^{14}
Cu-Cl (ψ_1)	-6.13×10^{14}
d_{xz}	2.32×10^{14}
d_{yz}	-1.16×10^{14}
d_{xy}	-1.16×10^{14}

TABLE XXIX

Estimated Orbital Populations and Charge Densities

	No - $d\pi$ - $d\pi$ bonding	with $d\pi$ - $d\pi$ bonding
ψ_1	0.87	0.87
ψ_2	0.87	0.87
ψ_3	0.87	0.87
ψ_4	0.70	0.70
$\delta^+(S_1)$	0.87	0.37
$\delta^+(S_2)$	0.87	0.37
$\delta^+(S_3)$	0.87	+0.37
$\delta^-(Cl)$	-0.3	-0.3
$\delta^-(Cu)$	-2.31	-1.31
π_1	-	0.5
π_2	-	0.5

Again, the ionic contribution of the sulfur and chlorine atoms must be considered. The ionic contributions to $q)_{zz}$ are calculated by using the same procedure used for $Cu(tu)_2Cl$ and are tabulated in Table XXXI.

The observed EFG-Z components due to ions is related to the calculated value as follows:

$$q_{zz})^{ionic}_{obs} = q^{ionic}_{cal}\ (1-\gamma_{\infty})$$
$$= 18 \times (-0.764)$$
$$= -13.75 \times 10^{14}\ esu/cm^3$$

For no $d\pi - d\pi$ and -7.9×10^{14} esu/cm^3 for $d\pi - d_{\pi}$ respectively. The nuclear quadrupole coupling constant due to both ionic and covalent contributions is

$$e^2Qq)_{obs} = e^2Qq\ (q^{ionic}_{obs} + q^{cov}_{obs})$$
$$= \frac{4.8 \times 10^{10} \times 0.16 \times 10^{-24}\ (-13.73 - 1.13)}{6.627 \times 10^{-27}}$$
$$= -17.27\ MHz$$

for no $d\pi - d\pi$ and -10.45 MHz for $d\pi - d\pi$ respectively. These estimated values are considerable lower than the experimentally observed value, 77.6 MHz. The reason for the difference is not yet known. Further information regarding the details of the crystal structure is needed before any conclusions can be drawn.

C) Molybedenum Oxyhalides

Table XVII tabulated the observed frequencies for Mo^{95} or Mo^{97} along with the observed Cl^{35} frequencies for $MoOCl_4$ and MoO_2Cl_2. For one of the Mo isotopes, both of which have a nuclear spin, I=5/2,

TABLE XXX

Ionic Contribution of Cl, S and Cu to q_{zz})

	with no -d -d	with -d -d
$\delta^+(S_1)$	-0.186×10^{14} esu/cm^3	-0.079×10^{14} esu/cm^3
$\delta^+(S_2)$	-0.186×10^{14} esu/cm^3	-0.079×10^{14}
$\delta^+(S_3)$	-0.186×10^{14} esu/cm^3	-0.079×10^{14}
$\delta^-(Cl)$	-0.204×10^{14} esu/cm^3	-0.204×10^{14}
d_{xy}	$+4.64 \times 10^{14}$	$+3.48 \times 10^{14}$
d_{yz}	-2.32×10^{14}	-1.74×10^{14}
d_{xz}	-2.32×10^{14}	-1.74×10^{14}
d_{z^2}	-4.64×10^{14}	-4.64×10^{14}
$d_{x^2-y^2}$	$+4.64 \times 10^{14}$	$+4.64 \times 10^{14}$
Total	-0.764×10^{14}	-0.441×10^{14}

the values of $(e^2Qq)_{zz}$ and η were obtained from the experimental frequencies by use of the series approximation for the transition frequencies given in Table II. NMR studies [54] have shown the ratio of the moments, Mo^{95}/Mo^{97} to be equal to 9.3. From this ratio and the observed Mo frequencies, one should expect to observe the other pair of frequencies at either approximately 300 MHz or 3 MHz, both of which are beyond the operating range of the spectrometer. The assignment of the observed frequencies to a particular isotopic species is therefore impossible at the present time. We have also investigated a number of other Mo-compound and were unable to observe any resonances. The limited number of observation severely restrict the discussion of any relationships of the observed frequencies to the bonding properties. We have, however opened up an interesting field for further studies.

BIBLIOGRAPHY

1. H. A. Bent, Chem. Rev., 61, 290 (1961).

2. R. Bersohn, J. Chem. Phys., 20, 1505 (1952).

3. T. L. Brown, P. A. Edwards, C. B. Harris and J. L. Kirsch, Inorg. Chem., 8, 763, 1969.

4. C. Sharpe Cooke, Structure of Atomic Nuclei (D. van Nostrand Co., Inc., New York, 1964).

5. Cohen, M. H., Physical Rev., 96, 1278 (1954).

6. R. Croston, "Noise Control and Frequency Measurement of the Super-regenerative Nuclear Quadrupole Spectrometer," M.S. Thesis, West Virginia University (1967).

7. Das, T. P. and E. L. Hahn, "Nuclear Quadrupole Resonance Spectroscopy", Academic Press, New York, 1958.

8. Dean, C., Thesis, Harvard University through ref. 6.

9. M. A. El-Sayed and H. D. Kaesz, J. Mol. Spectro., 8, 310 (1962).

10. N. Flitcroft and H. D. Kaesz, J. Am. Chem. Soc., 85, 1377 (1963).

11. Gordy, W., "Quadrupole Coupling, Dipole Moments and the Chemical Bond", Discussion Faraday Soc., 19, 14, (1955).

12. Gordy, W., W. V. Smith and R. F. Trambarlo, "Microwave Spectroscopy", John Wiley, New York (1951).

13. Gordy, W., "Interpretation of Nuclear Quadrupole Coupling in Molecules", J. Chem. Phys., 17, 792 (1951).

14. Graybeal, J. D. and C. D. Cornwell, "Nuclear Quadrupole Spectra of the Choloroactonitriles", J. Phys. Chem., 62, 483, (1958).

15. Heiber A.J., J. Am Chem. Soc., 83, 1387 (1961

16. W. A. G. Graham, Inorg. Chem., 7, 315 (1968).

17. J. R. Holms and H. D. Kaesz, J. Am. Chem. Soc., 83, 3903 (1961).

18. W. Jetz, P. B. Simmon, J. A. J. Thompson and W. A. G. Graham, Inorg. Chem., 5, 2217, 1966.

19. W. Jetz and W. A. G. Graham, J. Am. Chem. Soc., 89, 2773 (1967).

20. Kauzmann, "Quantum Chemistry", Academic Press, Inc., New York, New York, 1957, p. 333, 8731.

21. Knobler, C. B., Yokazz and Pepinsky, Z. Krist., 111, 385 (1959).

22. Kohlschuller, V., Ber., 36, 1151, (903).

23. V. S. Korol'kov and A. G. Makhenek, opt. spektrask, 12, 87 (1962).

24. Kuncher, N. R. and M. R. Truler, J. Am. Chem. Soc., 80, 3478 (1958).

25. Lane, T. J., D. N. Sen and J. V. Ouagliano, J. Chem. Phys., 22, 1885 (1954).

26. R. Livingston and H. Zeides, ORNL-1913, 1955.

27. E. A. C. Lucken, "Nuclear Quadrupole Coupling Constants", Academic Press, Inc., 1969.

28. McKnown, G.L., "Nuclear Quadrupole Resonance Zeeman Spectra of $KCu(CN)_2(I)$, Ph.D. Thesis (1965), West Virginia University.

29. McKnown, R. J., Ph.D. Thesis, West Virginia University.

30. H. R. H. Patil and W. A. G. Graham, J. Am. Chem. Soc., 87, 673, (1965).

31. H. R. H. Patil and W. A. G. Graham, Inorg. Chem., 5, 1401 (1966).

32. D. J. Patmore and W. A. G. Graham, Inorg. Chem., 5, 1586 (1966).

33. D. J. Patmore and W. A. G. Graham, Inorg. Chem., 5, 2222, (1966).

34. D. J. Patmore and W. A. G. Graham, Inorg. Chem., 5, 1405, (1966).

35. D. J. Patmore and W. A. G. Graham, Inorg. Chem., 6, 981, (1967).

36. D. J. Patmore and W. A. G. Graham, Inorg. Chem., 7, 771, (1968).

37. D. J. Patmore and W. A. G. Graham, Inorg. Nucl. Letters, 2, 179 (1966).

38. Pauling, L., "Nature of the Chem. Bond," Cornell University Press, Ithaca, New York, 1939.

39. Pratorius-Seidler, G., Prakt. Chem., 21, 129 (1880).

40. Rathke, B., Ber., 14, 1774 (1884).

41. Rathke, B., Ber., 17, 1294 (1884).

42. Ramsay, N. T., "Nuclear Moments", John Wiley and Sons, Inc., New York, 1953.

43. A. H. Reddoch, Atomic Energy Comm., reported UCRL, 8972, 1959.

44. Rosenheim, A. and W. Lowenslainum, Z. Anorg. U. Allegem. Chem., 34, 62 (1903).

45. P. L. Simmons and W. A. G. Graham, J. Organometallic Chem., (Amsterdam), 8, 479 (1967).

46. A. F. Schreiner and T. L. Brown, J. Am. Chem. Soc., 90, 3366 (1968).

47. Diane D. Spencer, J. L. Kirsch and T. L. Brown, Inorg. Chem., (1970).

48. W. A. Spofford, Text and E. L. Amma, Chem. Comm., 405, 1968.

49. W. A. Spofford, Text and E. L. Amma, Acta Cryst., B26, 1474, 1970.

50. Swaminathan, K. and H.M.N.H. Irving, J. Inorg. Nucl. Chem., 26, 1291 (1964).

51. E. Swiger and G. L. McKnown, 22nd Richmond Region ACS Meeting.

52. J. A. J. Thompson and W. A. G. Graham, Inorg. Chem., 6, 1365 (1967).

53. C. H. Townes and B. P. Darley, J. Chem. Phys., 17, 782, (1949).

54. C. H. Townes and A. L. Schawlow, "Microwave Spectroscopy", McGraw Hill, New York, 1955.

55. Urenka, R. G. and E. L. Amma, J. Am. Chem. Soc., 58, 4270 (1966).

56. Vizzini, E. A. and E. L. Amma, Dissertation Abstra., 23, 3654 (1963).

57. R. E. Watson and A. J. Freeman, Phys. Review, 131, 250 (1963).

58. Yamazuchi, A., R. B. Penland, S. Mizuchima, T. J. Lane, C. Curran, and T. V. Quagliano, J. Am. Chem. Soc., 80, 527 (1958).

The vita has been removed from the scanned document

ABSTRACT

The work described in this dissertation represents an effort to extend the application of Nuclear Quadrupole Resonance spectroscopy to the study of transition element compounds. Using a conventional noise controlled superregenerative spectrometer compounds of cobalt, copper and molybdenum have been investigated.

Three biscobalt(tetracarbonyl) tin(II) compounds were investigated and the ^{59}Co resonances measured in each. Each compound exhibited a doublet indicative of two crystallographic inequvilent sites. The asymmetry parameters were all between 0.005 and 0.10 indicating little distortion of the cobalt enviroments from the expected C_{3v} symmetry. The coupling constants as obtained by use of a series approximation for the transition frequencies and confirmed by a frequency ratio plot were $Cl_2Sn[Co(CO)_4]_2$ -146.9MHz, $(C_6H_5)ClSn[Co(CO)_4]_2$ -137.7 MHz, $(C_6H_5)_2Sn[Co(CO)_4]_2$ -112.9 MHz. The observed coupling constants correlate with the inductive effects of the substitutents in the tin.

The study of several Copper(I) coordination compounds represents the first known attempt at using Cu nuclear quadrupole coupling constants to study onding in a situation other than an isolated compound. Assuming zero asymmetry parameters the following ^{63}Cu coupling constants were observed; $Cu(tu)_2NO_3$- 50.18 MHz, $Cu(tu)_2Cl$ - 41.41 MHz, $Cu(tu)_2Br$- 32.62 MHz, $Cu(etu)_2ClO_4$- 45.76 MHz, $[Cu(etu)_4]_2SO_4$- 63.12 MHz, $Cu(etu)_2Cl$ - 55.72 MHz, $Cu(etu)_2Br$- 64.02 MHz, $Cu(dmtu)_3Cl$ - 77.60MHz. The ligands used were tu=thiourea, etu=ethylene thiourea, and dmtu= N,N' dimethylthiourea. The crystal structures of only $Cu(tu)_2Cl$ and

$Cu(dmtu)_3Cl$ are known making direct comparison difficult. The general increase of the coupling constants with ligand substitution correlates with the partial charge on the sulfur atom of the free ligand. The reversal of the order of the coupling constants between the thiourea and ethylen thiourea halides indicates an an appreciable ion contribution to the coupling constant from the halogen. The observation of ^{79}Br resonance at 38.83 MHz in $Cu(etu)_2Br$ also confirms this point. By using sp^2 and sp^3 hybridization schemes for $Cu(tu)_2Cl$ and $Cu(dmtu)_3Cl$ the coupling constants were calculated to be 36.0MHz and 17.27 MHz respectively. This represents resonable agreement in view of the uncertainties in the Sternheimer factor used and the approximate nature of the model. The allowance for $d_{\pi} - d_{\pi}$ bonding between the Cu and S atoms decreases the calculated constants indicating that such bonding probably is of little importance.

Resonance were observed for Mo isotope in both $MoOCl_4$ and MoO_2Cl_2. Both possible Mo resonances as well as the Clresonances were observed. The particular isotope to which the resonances belong is as yet undetermined since those belonging to the other Mo isotopes with $I = 1$ will be outside the range of available instrumentation.